

Deciphering Temperature Seasonality in Earth's Ancient Oceans

Linda C. Ivany¹ and Emily J. Judd²

¹Department of Earth and Environmental Sciences, Syracuse University, Syracuse, New York, USA; email: lcivany@syr.edu

²Department of Paleobiology, Smithsonian National Museum of Natural History, Washington, DC, USA

Annu. Rev. Earth Planet. Sci. 2022. 50:123–52

First published as a Review in Advance on
December 9, 2021

The *Annual Review of Earth and Planetary Sciences* is
online at earth.annualreviews.org

<https://doi.org/10.1146/annurev-earth-032320-095156>

Copyright © 2022 by Annual Reviews.
All rights reserved

Keywords

paleoclimate, seasonality, sclerochronology, stable isotope, sea surface temperatures, model

Abstract

Ongoing global warming due to anthropogenic climate change has long been recognized, yet uncertainties regarding how seasonal extremes will change in the future persist. Paleoseasonal proxy data from intervals when global climate differed from today can help constrain how and why the annual temperature cycle has varied through space and time. Records of past seasonal variation in marine temperatures are available in the oxygen isotope values of serially sampled accretionary organisms. The most useful data sets come from carefully designed and computationally robust studies that enable characterization of paleoseasonal parameters and seamless integration with mean annual temperature data sets and climate models. Seasonal data sharpen interpretations of—and quantify overlooked or unconstrained seasonal biases in—the more voluminous mean temperature data and aid in the evaluation of climate model performance. Methodologies to rigorously analyze seasonal data are now available, and the promise of paleoseasonal proxy data for the next generation of paleoclimate research is significant.

- The seasonal cycle defines climate and its constraints on biology, both today and in the deep past.
- Paleoseasonal data improve proxy-based estimates of mean annual temperature and validate Earth System Model simulations.

ANNUAL
REVIEWS **CONNECT**

www.annualreviews.org

- Download figures
- Navigate cited references
- Keyword search
- Explore related articles
- Share via email or social media

- Large, internally consistent data sets can reveal robust spatiotemporal climate patterns on the ancient Earth and how they change with $p\text{CO}_2$.
- Computational tools enable rigorous numerical analysis of paleoseasonal data for comparison with other paleoclimate data and model output.

INTRODUCTION

Anthropogenic climate change is one of the most pressing problems of the modern world. While this warming is most frequently discussed in terms of global mean surface temperature (e.g., the 2°C warming threshold above preindustrial values), the effects of climate change are ultimately experienced on a seasonal scale (Matthews et al. 2016). Changes to the frequency and intensity of drought, forest fires, floods, growing seasons of vital crops, and extreme weather events all have a direct impact on humans. Biology on the whole, too, responds not to changes in average temperature but to changes in the extremes, which interact with other variables to place limits on where taxa can exist both on land and in the sea (Ljungström et al. 2021, Sunday et al. 2012, Valentine 1983). As recent heat waves in Australia and the North American Pacific Northwest demonstrate, with small changes in global mean temperature can come large changes in seasonal extremes and their variability, resulting in dramatic consequences for people and ecology.

Understanding how the seasonal cycle will change in response to global warming is therefore of paramount importance. Tackling this question requires two strategies: forecasting with climate models (Meehl et al. 2021, Roy et al. 2020) and drawing insights from past warm climates (Burke et al. 2018, Tierney et al. 2020a). As the closest analogs for our near future are being pushed farther back in geologic time, paleoclimate data from deep-time settings are becoming more and more important—accurate assessment of Earth’s ancient temperatures is no longer simply an academic pursuit. Much progress has been made on understanding past changes in mean annual temperature (MAT), but paleoclimate research often neglects how seasonal extremes and their variability differed in, for example, the high- CO_2 Eocene world in comparison to today. Seasonally resolved proxy records collected within a framework that allows for hypothesis testing and quantitative evaluation are essential to pair with MAT data and Earth System Model (ESM) simulations to both better understand surficial dynamics and formulate predictions about the future. Indeed, climate itself is defined by the annual cycle of the variables that comprise it (Carré & Cheddadi 2017), and changes in seasonality underpin how changes in MAT are brought about. Nevertheless, despite its intrinsic value, the seasonal cycle is only occasionally mentioned and rarely constrained in paleoclimate studies (Figure 1).

We argue that a concerted research effort should be devoted to characterizing the seasonal regime during key intervals and in key regions on the ancient Earth. Integral to this effort is the development of thoughtful and premeditated study designs and statistically and computationally rigorous data processing methodologies that enable robust evaluation of seasonal proxy data in a broader context. Knowledge of winter and summer temperatures sharpens existing estimates of MAT and can identify otherwise unrecognized seasonal biases in existing data. The annual temperature cycle is generated by ESMs, so even a few well-constrained proxy data can prove useful for validating model simulations. Critically, the effects of climate change on the biota are easier to interpret or predict when seasonal information is available—in both the past and the future. The growing awareness of the importance of seasonal data in the new generation of paleoclimate research, and for making climate change relevant to policy makers and the public, is a call to action for the proxy community.

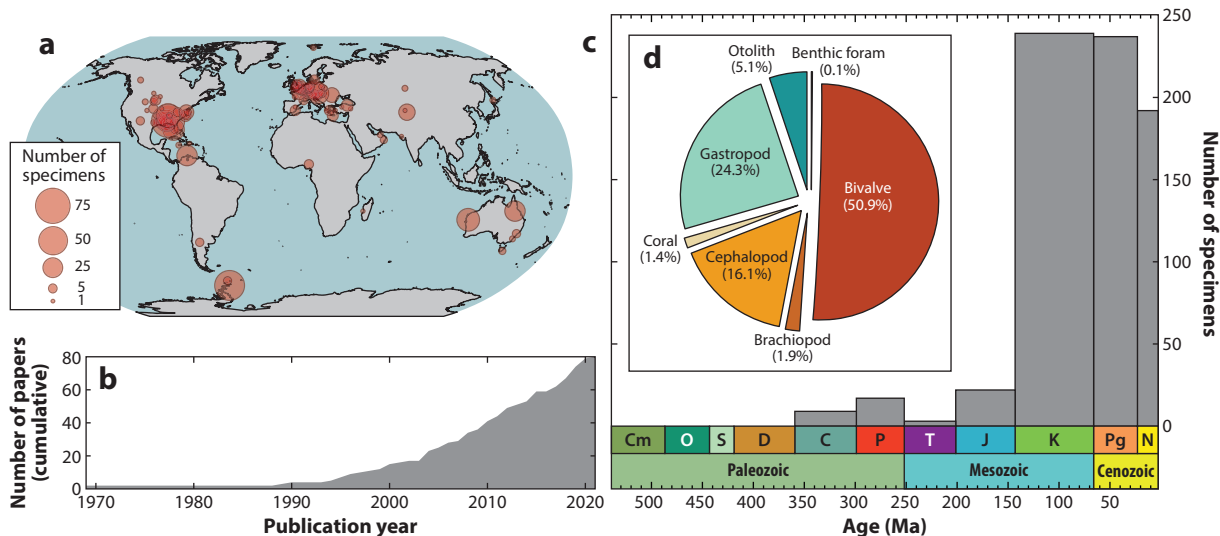


Figure 1

(a) Modern geographies of the locations for which there are paleoseasonal data, scaled by the number of specimens per site. (b) Cumulative number of publications containing paleoseasonal data through time. (c) Number of specimens for which there are paleoseasonal data through the Phanerozoic. (d) Breakdown of paleoseasonal specimens by taxon. Abbreviations: C, Carboniferous; Cm, Cambrian; D, Devonian; J, Jurassic; K, Cretaceous; N, Neogene; O, Ordovician; P, Permian; Pg, Paleogene; S, Silurian; T, Triassic.

Here we review the approaches used to extract and interpret records of paleoseasonality in Earth's deep past, ways to facilitate their incorporation into broader integrated studies that can interface with climate models, and the significant promise they offer for novel insights into the ancient—and future—Earth system. While seasonally resolved data are available from both continental and marine paleosettings, we focus here on seasonal sea surface temperature (SST) records for three reasons. First, continental temperatures depend heavily upon elevation, a variable difficult to constrain in the rock record (Botsyun & Ehlers 2021). In combination with elevation effects, variation in land surface cover and hence albedo (Kung et al. 1964) gives rise to spatiotemporal temperature heterogeneity that makes the limited paleodata difficult to interpret in a broader zonal, global, or temporal context. Finally, because ESMs that simulate the seasonal cycle yield predictions for how seasonality varies over the whole Earth surface, proxy-validated model estimates of marine seasonal SSTs should also be coupled with more reasonable estimates of continental temperatures. This review is further focused on the oxygen isotope values of sequentially sampled, accretionary biogenic materials. While a number of other paleotemperature proxy systems are now available, most either require taxon-specific calibrations or simply lack seasonal resolution.

SEASONALITY IN THE MODERN OCEAN

The term seasonality refers to variation in any property that exhibits a cyclic component with a period of 1 year. From a climatological perspective, seasonality is generally discussed as the mean annual range of temperature (MART) and is typically reported as the amplitude of the mean monthly temperature cycle averaged over at least 30 years.

The first-order variable influencing the seasonal range of temperature is the amount of solar radiation received at the surface. Milankovitch cyclicity in Earth's orbit gives rise to periodic changes in insolation (and seasonality) that ultimately drive climate change on a range of timescales (Westerhold et al. 2020). The interaction of orbital parameters and latitude combine to yield sinusoidal intra-annual variation in insolation at the top of the atmosphere. Air temperatures at the surface track this, modified by the effects of albedo and heat capacity, with a lag of roughly 1 month. SSTs follow in kind, except where formation of sea ice limits cooling below about -1.7°C , and they lag behind insolation by about yet another month (Prandle & Lane 1995, Rayner 2003). Because water has a higher heat capacity than land, marine settings experience smaller seasonal fluctuations in temperature than continents (Crowley et al. 1986). Regional and zonal variability in this value is largely driven by surface dynamics, suggesting that spatial patterns may provide insight into ancient circulation patterns (Judd et al. 2020). Marine MART is also modulated by the regional effects of stratification.

In today's ocean (**Figure 2**), seasonality of SSTs exhibits minima near the equator, where insolation is high all the time, and near the poles, where water stays cold all the time. Seasonal range increases moving away from the equator as winter and summer insolation diverge. Unlike air temperatures, which continue to diverge toward the poles because of cold, dark winters, seasonal range in SST actually decreases from the midlatitudes toward the poles, as summers cool while winter temperatures become increasingly constrained by the freezing point of seawater. Greater landmass coverage in the Northern Hemisphere gives rise to hemispherically asymmetric peaks in seasonal range (Jain et al. 1999, Jones et al. 1999) (**Figure 2b**). High northern latitude landmasses amplify seasonality by promoting the development of strong subtropical high-pressure cells, which modulate seasonal temperature differences especially in western boundary current regimes, whereas the continuous expanse of the Southern Ocean results in homogenization and attenuation of SST seasonality in high austral regions (Judd et al. 2019, Seager et al. 2003). Nearly everywhere, seasonal variation is well approximated by a sinusoid with period of 1 year, consistent with variation in insolation, and exceptions are geographically nonrandom (**Figure 2c**): In the tropics, convection associated with movement of the intertropical convergence zone dominates over the insolation signal, and freezing truncates winter SST variation near the poles. The degree to which the present distributions of mean and seasonal temperatures have characterized Earth's past, with changing greenhouse gas concentrations and tectonic configurations, is a first-order question that drives much ongoing paleoclimate research (Burke et al. 2018, Tierney et al. 2020a, Westerhold et al. 2020).

ARCHIVES OF TEMPERATURE PALEOSEASONALITY AND HOW TO ACCESS THEM

Temperature-sensitive fossils and lithologies provide insight into the climate regime at the time of deposition based on an understanding of physiology and modern occurrence distributions, but quantitative measures of paleo-SSTs nearly all derive from temperature-dependent aspects of the chemistry of biomaterials and minerals that precipitate on Earth's surface. The oxygen isotope ($\delta^{18}\text{O}$) and clumped isotope (Δ_{47}) values of carbonates and phosphates, Mg/Ca ratios of select carbonates, and molecular properties of several biomarkers (e.g., TEX₈₆, alkenones) have been linked to ambient temperature with a high degree of confidence (see the sidebars titled Proxy Systems: Oxygen Isotope Ratios, Proxy Systems: Clumped Isotopes, Proxy Systems: Elemental Ratios, and Proxy Systems: Biomarkers). In the absence of additional information, data are typically interpreted in the context of MAT, although there is growing acknowledgment of the potential for seasonal bias (e.g., Dolman et al. 2021). Seasonality itself, however, is a difficult variable to

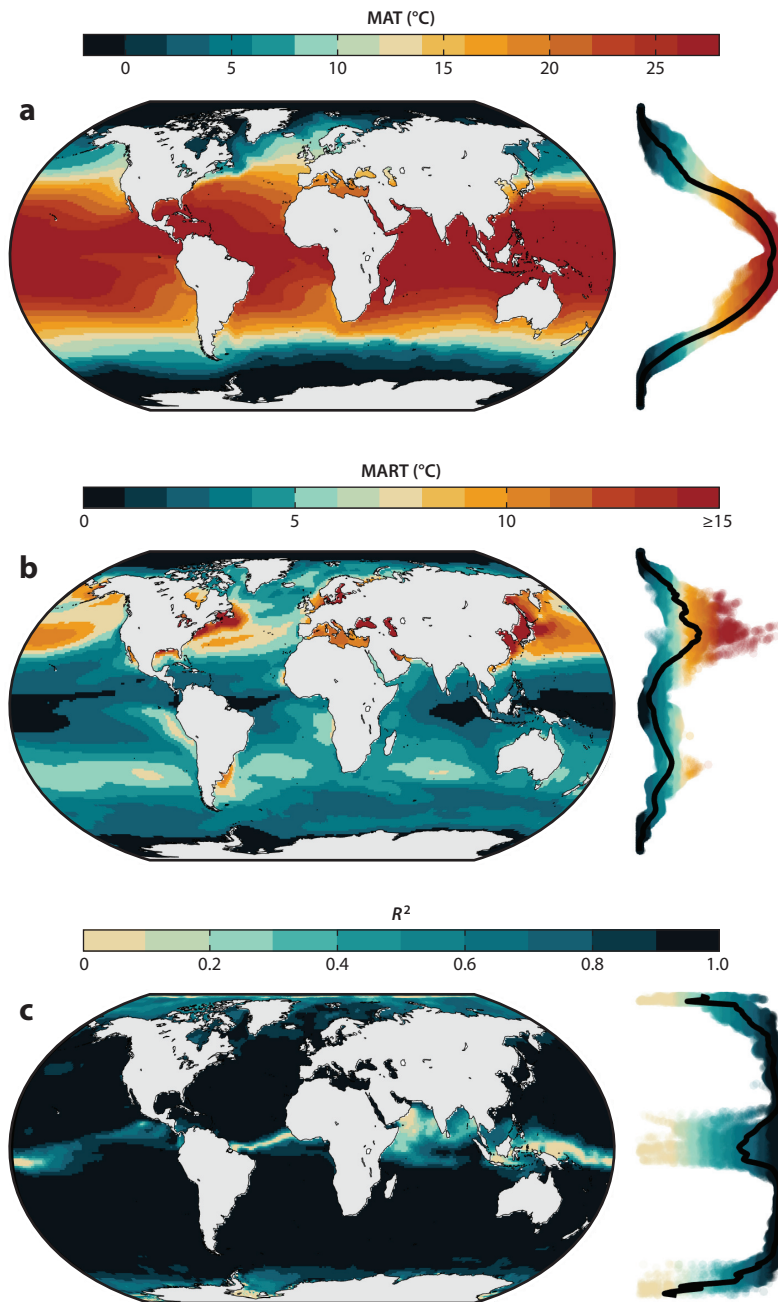


Figure 2

Maps showing the spatial distribution of (a) the MAT, (b) the MART, and (c) the adjusted R^2 value of the mean monthly values fit with a sinusoid with a fixed period of 12 months. Data on the right show patterns in the relative spread of values (color coded) and the mean latitudinal value (black line). Abbreviations: MART, mean annual range of temperature; MAT, mean annual temperature; R^2 , coefficient of determination. Sea surface temperature data from Hirahara et al. (2014).

PROXY SYSTEMS: OXYGEN ISOTOPE RATIOS

The ratio of ^{18}O to ^{16}O of carbonate (or other minerals) is a function of both the temperature at the time of precipitation and the oxygen isotope ratio of the water from which the carbonate precipitates (Urey 1948). The degree of fractionation between the heavy and light isotopes increases with decreasing temperature, and equilibrium relationships are well understood based on both experimental and empirical calibration studies, giving rise to the temperature equations that have been the backbone of paleoclimate research for many decades (see reviews by Grossman 2012, Pearson 2012). Oxygen isotope values are reported in delta notation ($\delta^{18}\text{O}$), reflecting the deviation of the ratio from a standard. $\delta^{18}\text{O}$ values can be determined with very high confidence (typically well below 0.1 per mil) from very small sample sizes (15–20 μg), enabling subseasonal resolution from many accretionary materials. At present, sequential $\delta^{18}\text{O}$ analysis of accretionary materials is the only way to consistently capture paleoseasonal temperature variation from accretionary proxy materials. Dependence of the system on $\delta^{18}\text{O}$ of the seawater ($\delta^{18}\text{O}_{\text{sw}}$) does, however, introduce significant uncertainty in deep-time paleotemperature estimates, as this value is often poorly constrained (see the section titled Translation to Paleotemperatures).

PROXY SYSTEMS: CLUMPED ISOTOPES

Carbonate clumped isotope paleothermometry relies on the thermodynamically constrained, temperature-dependent propensity for the minor isotopes of ^{18}O and ^{13}C to bond or “clump” together in the carbonate lattice more readily at cooler temperatures. Because clumped isotope values (Δ_{47}) are calculated by comparing the observed proportion of clumped molecules ($^{18}\text{O}^{13}\text{C}^{16}\text{O}$, with mass 47) in the sample to that of a stochastic distribution of isotopes in the same sample, the measure is independent of the $\delta^{18}\text{O}$ of seawater ($\delta^{18}\text{O}_{\text{sw}}$) (Affek 2012, Eiler 2011), alleviating the need to make assumptions. While this offers considerable advantages over $\delta^{18}\text{O}$ -based paleothermometry, the measure is still subject to all the same diagenetic concerns associated with dissolution and reprecipitation, and importantly, also to diffusion-driven solid-state bond reordering (Passey & Henkes 2012), the degree of which is thus far impossible to detect in geological materials and can be modeled based only on presumed burial/heating history (Hemingway & Henkes 2021). Sizable analytical uncertainties and the need for large sample sizes limit the direct use of Δ_{47} in most paleoseasonal studies, but like Mg/Ca ratios, it can provide the constraints on the $\delta^{18}\text{O}_{\text{sw}}$ necessary for calculating high-resolution $\delta^{18}\text{O}$ -based temperatures.

PROXY SYSTEMS: ELEMENTAL RATIOS

The Mg/Ca ratio of calcite produced inorganically and by organisms such as planktonic and benthic foraminifera and ostracods increases with temperature (Lea 2014, Lea et al. 1999, Lowenstein & Hönisch 2012). Calibration equations are taxon specific and rely on estimates of the Mg/Ca ratio of seawater, which changes over the Phanerozoic, but foraminifera are widely used to provide constraints on paleo-sea surface temperatures in the late Mesozoic and Cenozoic, thus enabling calculation of the $\delta^{18}\text{O}$ of seawater from the $\delta^{18}\text{O}$ values of the same carbonate (Lear et al. 2000) (see the section titled Translation to Paleotemperatures). Strong physiological controls on the incorporation of minor elements into the skeletons of accretionary macrofossils, which record seasonality, generally obviate universal calibrations and hence make them difficult to interpret in a paleotemperature context (Gillikin et al. 2005, Pérez-Huerta et al. 2008, Poulain et al. 2015, Schöne et al. 2011). Nevertheless, taxon-specific Sr/Ca ratios in corals can provide independent control on mean annual temperature (DeLong et al. 2013, Marshall & McCulloch 2002), although preservation often limits these records to the Quaternary.

PROXY SYSTEMS: BIOMARKERS

The properties of select organic molecules produced by marine plankton are known to exhibit relationships to water temperature at the time of growth. The proportions of unsaturated ketones in alkenones produced by haptophyte algae vary consistently such that the $U_{37}^{K'}$ unsaturation index increases with temperature (Brassell et al. 1986, Herbert 2014). Similarly, membrane lipids produced by marine Archaea contain more cyclopentane rings at warmer temperatures, leading to development of the TEX₈₆ paleotemperature proxy (Inglis & Tierney 2020, Schouten et al. 2002). Alkenones are most useful in sediments of Eocene age or younger, while TEX₈₆ has been applied back into the Mesozoic. Both metrics saturate at warmer temperatures, with the latter having a greater range. The relevant organic molecules appear to be comparatively insensitive to diagenetic alteration and are especially useful in sediments lacking well-preserved carbonates. Like proxies derived from mineralized microfossils, these molecules are produced by short-lived plankton analyzed in aggregate, and hence the metrics are best interpreted as proxies for mean annual temperature at the sea surface, although reconstructed temperatures may be affected by the depth at which the organisms lived and/or seasonal bias in production.

quantify in deep time. While insights can be drawn from proxy materials known to consistently form in one seasonal extreme or another [which itself is difficult to establish (e.g., Kelson et al. 2020)], sedimentary archives generally cannot provide a coherent record of the full range of temperatures expressed during the annual cycle. Rapidly accumulating sedimentary materials such as speleothems (Baldini et al. 2021), tufa (Matsuoka et al. 2001), and varved deposits (Zander et al. 2021) can provide impressively long annually resolved records, but the intra-annual signal is often restricted to an on-off or high-low pattern with no clear chronometer, and most are restricted to relatively recent and terrestrial settings. The fossil record, however, is replete with seasonally growing marine plankton and multiyear accretionary skeletons, the geochemical properties of which chronicle ancient seasonal regimes.

Paleontological Recorders

Paleontologists have long known that temperature affects the distribution and growth of organisms. Some taxa are constrained by their physiologies to particular windows of temperature defined by seasonal extremes, so their presence in fossil assemblages can set limits on the conditions that existed at the time (e.g., Markwick 1998). Transfer functions based on assemblage composition are widely used paleoclimate proxies, and some of these also estimate seasonal extremes (CLIMAP 1981, Pisias et al. 1997). Because these approaches are based on taxon occurrences, they are not subject to the diagenetic concerns that permeate the geochemical studies on which this review is focused, but they do rely on assumptions of taxonomic uniformity in relation to climate, making them increasingly uncertain or altogether unavailable in the very distant past.

While the identity of fossils is useful, their chemistries have become much more so. Geochemical paleothermometers applied to biogenic materials are now the mainstay of deep-time paleoclimate research. Data derived from planktonic and benthic biomineralizers and organic-walled microfossils collected across the world's oceans by, for example, the Integrated Ocean Drilling Program (IODP) span the Jurassic to Recent. The bulk of these data represent time-integrated samples containing many individuals each and hence more accurately approximate MAT, but most marine protists individually have lifespans of weeks to months, so their biomaterials have the potential to capture seasonally relevant information. The range in proxy temperature values extracted from a number of individual planktonic microfossils can approximate the seasonal SST range for a given time slice, provided that growth occurs year-round and

interannual variation can be deconvolved (Metcalf et al. 2019, Thirumalai et al. 2013, Wit et al. 2010). However, taxon-specific preference for growth during only one portion of the annual cycle and/or changes in depth preference, if not recognized, can lead to underestimates of seasonal range and biased estimates of MAT (Fraile et al. 2009, Groeneveld et al. 2019). These kinds of studies are the only ways to make inferences about the seasonal cycle from microfossils, from which the bulk of Meso–Cenozoic paleoclimate records derive.

For all the richness of information gleaned from the array of temperature proxies as applied to microfossils and biomarkers, neither they nor their sedimentary accumulations can provide data with the temporal resolution sufficient to resolve continuous intra-annual records of temperature. The mineralized hard parts of accretionary marine macrofauna, however, grow more or less continuously over the course of their lives (see the extensive literature on sclerochronology, e.g., Pannella & MacClintock 1968 and papers in Rhoads & Lutz 1980); thus, they record in their chemistries a history of the temperatures experienced by the organism over time. High-resolution geochemical analysis along the growth trajectory can reveal this record (Jones 1983, Schöne & Surge 2012). The approach is not without its challenges, as discussed below, but provided the relationship between chemistry and temperature is understood and the material is not subsequently modified by diagenesis, accretionary skeletons from the fossil record provide critical seasonal information otherwise unavailable to paleoclimatologists. While we focus on the marine realm here, the approach also provides insight into the paleoseasonality of temperature and precipitation on continents.

Accretionary Skeletons: Considerations of Taxonomy, Ecology, and Preservation

The realization that accretionary skeletal materials can preserve a chemical record of paleoseasonality dates back to the formative days of oxygen isotope paleothermometry, when Urey and colleagues (1951) subsampled a Cretaceous belemnite and found regular variation in $\delta^{18}\text{O}$ values with growth that they interpreted as annual. The confluence of sclerochronology and oxygen isotope paleothermometry led to extensive work in the early 1980s exploring the ability of mineralized accretionary skeletons to record seasonal variations in water temperature, thereby providing access to ancient seasonal cycles using fossils (Arthur et al. 1983, Jones 1983, Rye & Sommer 1980, Williams et al. 1982). Since then, a range of living taxa have been shown to biomineralize in oxygen isotopic equilibrium with seawater, demonstrating their usefulness in a paleoclimate context (reviewed in Ivany 2012, Wefer & Berger 1991). Deviations from equilibrium are generally ascribed to so-called vital effects, the complex origins of which lie with factors such as extension rate, local pH, minor element concentration, and the behavior of carbonic anhydrase during precipitation (Brand et al. 2013, Chen et al. 2018, McConnaughey 1989).

Of the accretionary organisms, mollusks and articulate brachiopods are the taxa most often used to estimate MAT from $\delta^{18}\text{O}$ in deep time. Mollusks, especially bivalves, are employed far more often than brachiopods for seasonal studies because their growth bands, like tree rings, are more apparent and thus allow for high-precision spatial sampling (**Figures 1** and **3**). The calcite shells of brachiopods, however, are an underutilized resource for exploring seasonality in the Paleozoic. Both groups exhibit $\delta^{18}\text{O}$ values consistent with equilibrium precipitation, so long as adjustments are made for MgCO_3 in the shells of brachiopods (Brand et al. 2013). Immenhauser and colleagues (2016) present an excellent review of the ecology, biomineralization, and geochemistry relative to paleoenvironmental interpretation for both these groups. Corals can yield long records, but their calibration equations are taxon specific (Marshall & McCulloch 2002, McConnaughey 1989, Swart 1983), making their application in deep time challenging. The aragonite otoliths of fishes yield seasonal data important to fisheries and archeology (Campana 1999, Darnaude et al. 2014,

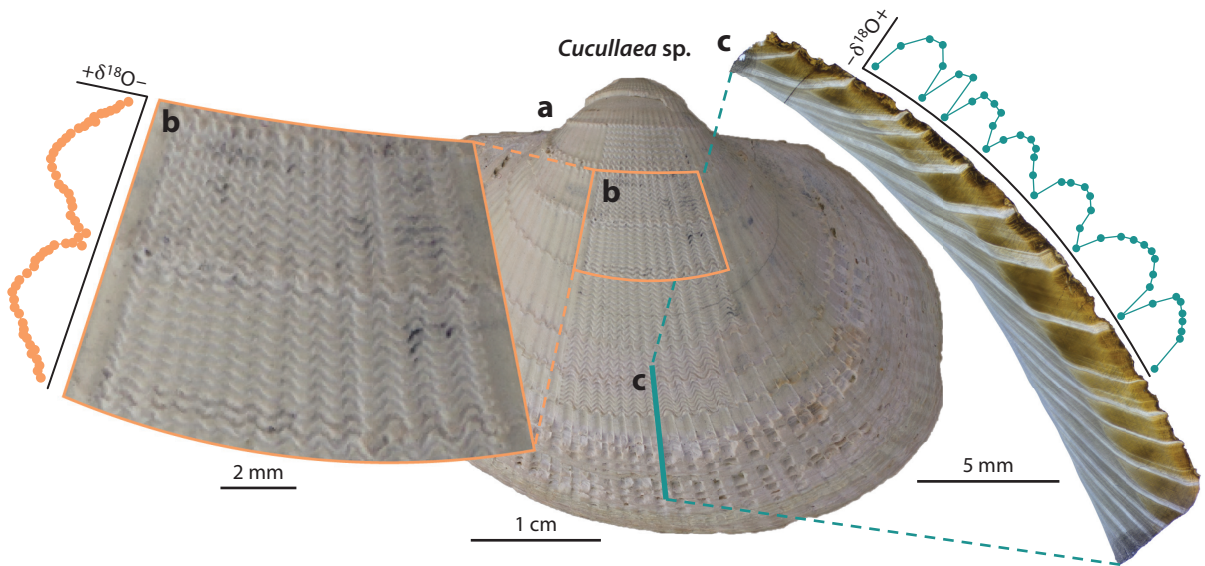


Figure 3

(a) The Eocene bivalve *Cucullaea* from Seymour Island, Antarctica, with close-ups showing the growth banding, sampling paths, and idealized isotope profiles from the cleaned exterior of the shell (b) and along a polished cross section of the shell (c).

Disspain et al. 2016, Radtke et al. 1996) as well as deep time (e.g., Ivany et al. 2000). And the $\delta^{18}\text{O}$ values and Mg/Ca ratios of carbonate in the tests of larger benthic foraminifera have been calibrated to temperature and can yield paleoseasonal records (Evans et al. 2013, Purton & Brasier 1999, Wefer & Berger 1980). While temperature calibration can be done only with living taxa, biomineralization processes largely hold true across members of a higher taxon, so equations determined in the Modern should hold true in deep time. Taxa from fully marine settings yield more straightforward $\delta^{18}\text{O}$ data than those from brackish settings, where there is large uncertainty about the composition and variability of $\delta^{18}\text{O}_{\text{sw}}$ (Ingram et al. 1996). Likewise, taxa that are less mobile—for example, many benthos—are more reliable than pelagic animals, whose potential for vertical or lateral movement in the water column can make isotope profiles difficult to interpret (Linzmeier 2019). Careful selection based on, and a priori knowledge of, the taxonomic identity and ecology of the biomineralizer being sampled minimizes error in the interpretation of skeletal isotope values.

Diagenesis can alter skeletal $\delta^{18}\text{O}$ values such that they no longer reflect the conditions at the time of growth. Proving retention of original composition is impossible, but careful screening of mineralogy, trace element chemistry, and shell microtextures bolsters confidence in paleotemperatures recovered from fossil materials (reviewed in Grossman 2012). The presence of seasonal variation suggests that at least some of the original biogenic signal has been preserved, but a number of processes can conceivably shift, attenuate, or exaggerate what was a primary cycle, and such alteration might be difficult to detect. Moon et al. (2021), for example, demonstrate retention of seasonal range in $\delta^{18}\text{O}$ and mineralogy despite a shift in overall isotope values associated with heat alteration. While discussion continues over the significance of proxy data from the Paleozoic, many now argue for the preservation of original isotopic compositions in select specimens back through the Phanerozoic (e.g., Brand 2004, Henkes et al. 2018, Veizer & Prokoph 2015), opening the door for paleoseasonal work in the very deep past.

GROWTH BANDING AND SKELETAL ACCRETION

Growth slowdowns or cessations give rise to growth banding, a feature nearly ubiquitous across taxa that grow by accretion (Kennish 1980, Lutz & Rhoads 1980). Annual bands are most common, and paired analyses of growth rate/banding profiles with instrumental data demonstrate that extension rates typically correlate with (often seasonal) variations in temperature (Jones & Quitmyer 1996), productivity (Witbaard et al. 2001), salinity (Addino et al. 2019), and/or the timing of reproduction (Sato 1995). Additionally, many organisms exhibit higher-order banding that forms on timescales ranging from circatidal (Schöne et al. 2002) to circalunidian (Miyaji et al. 2010), and analyses of these growth increments can provide insights into environment and ecology. For example, counts of daily bands in Devonian corals (Wells 1963) and Cretaceous oysters (Berry & Barker 1968) provided some of the first empirical evidence that the number of days in a year decreased over Earth's history. Growth profiles of daily bands indicate that extension rates increase approaching optimal conditions and slow with increasing stress. When environmental or physiological stress (e.g., during reproduction) is sufficiently high, growth can cease completely. High-latitude taxa are more likely to exhibit winter growth cessations; summer growth bands are less common but tend to occur in the subtropics (Killam & Clapham 2018).

Growth, Time, and Sampling Resolution

Changes in accretion rate are ubiquitous in biological materials, both intra-annually and over the lifespan of the organism (Lutz & Rhoads 1980) (see the sidebar titled Growth Banding and Skeletal Accretion). Therefore, equally spaced samples from an accretionary record collected along a growth axis will vary in the amount of time they represent (Beelaerts et al. 2010). Higher temporal resolution is possible early in ontogeny where growth is fastest and the record more expanded. As extension rate slows with age, time averaging increases and the recovered seasonal amplitude attenuates (**Figure 4a**). Likewise, preferential growth in one season over another decreases the number of samples and increases the time averaging of data from the season of least growth, giving rise to cusped isotope profiles that potentially underestimate the seasonal range (**Figure 4b**). Seasonal growth slowdowns tend to become more pronounced with age, and if growth stops altogether, the interval during which no shell is accreted can lengthen with age, both further decreasing seasonal amplitude. Goodwin et al. (2003) model various scenarios of slowing and seasonally truncated growth and present schematics to illustrate the expected patterns of isotope variation from serially sampled shells. Changes in growth rate, however, can largely be accommodated with the computational approaches discussed below.

Analytical Tools

Proxy-based paleothermometry traditionally requires physical sampling and subsequent analysis of sample powders. Sampling is done using a handheld drill or higher-precision computer-controlled milling system on either the cleaned exterior or polished cross section of the specimen (**Figure 3**). $\delta^{18}\text{O}$ values of the resulting carbonate powders are determined by isotope ratio mass spectrometry (IRMS). The ability to resolve seasonal cycles with confidence is limited by the ability to collect enough samples of sufficient size for geochemical analysis and with the requisite temporal resolution to reveal seasonal cycles. Development of an automated carbonate preparation system at Kiel University in the early 1980s paved the way to more quickly analyze the large numbers of samples required to document seasonal cycles, and the so-called Kiel device was subsequently optimized for small sample sizes (on the order of 15 μg) at the University of Michigan in 1986, making high-resolution studies involving hundreds of tiny samples more practical. Kiel

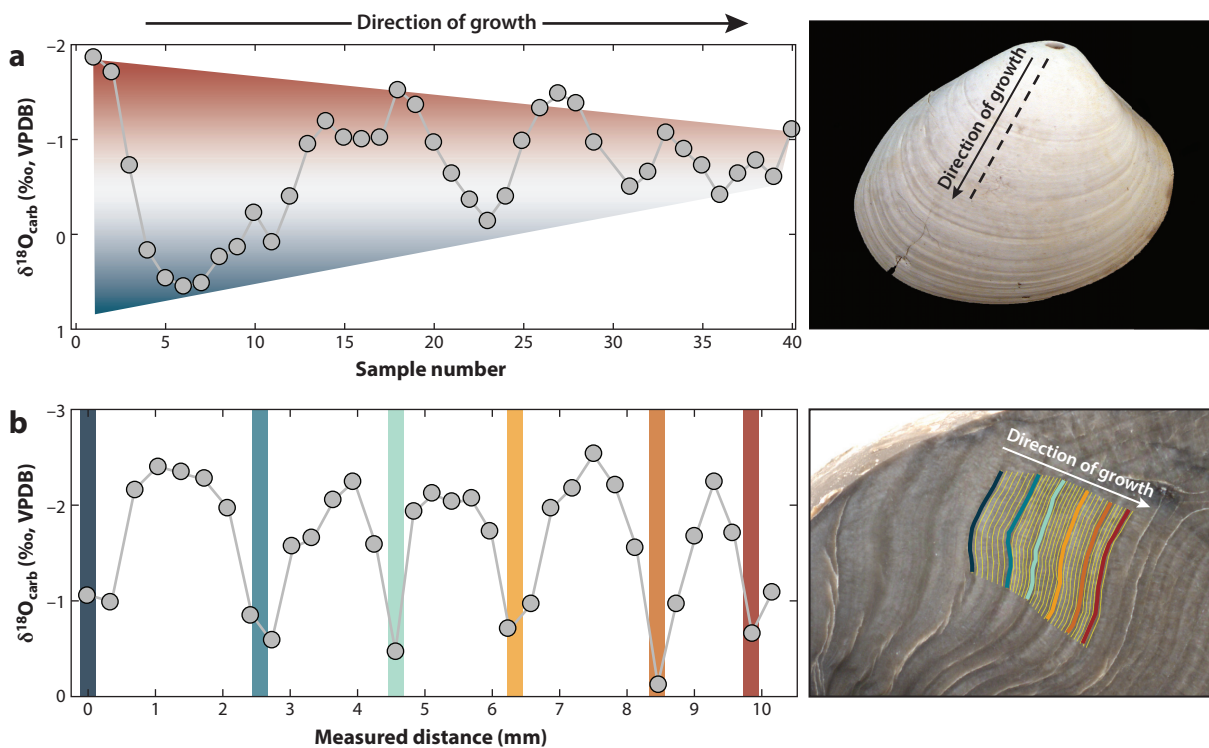


Figure 4

(a) Oxygen isotope profile of the Oligocene bivalve *Callista sobrina* showing the influence of decreasing growth rate on recovered seasonal amplitude across ontogeny (Ivany et al. 2004a). (b) Oxygen isotope profile of the early Permian bivalve *Eurydesma* showing the characteristic cusped pattern indicative of seasonal (winter) growth slow- or shutdown (Beard et al. 2015). Colored bars correspond with the positions of growth bands in the shell shown on the right, with all sampling paths. Abbreviations: $\delta^{18}\text{O}_{\text{carb}}$, $\delta^{18}\text{O}$ of carbonate; VPDB, Vienna Pee Dee Belemnite. Figure adapted from Ivany (2012).

devices are now being adapted for clumped isotope analyses as well (Meckler et al. 2014), once again easing sample size constraints and making high-resolution studies more feasible.

More recently, in situ compositional analysis has been made possible by laser ablation systems, secondary ion mass spectrometry (SIMS), micro-X-ray fluorescence (XRF), and synchrotron radiation, enabling even greater spatial precision in characterizing the variation preserved in accretionary records. While these are outstanding tools to reveal subannual variation in material properties, $\delta^{18}\text{O}$ values generated by these approaches may not be directly comparable to those generated by conventional IRMS (Edwards et al. 2022, Wycech et al. 2018). Nevertheless, the high spatial resolution afforded by these techniques enables seasonal reconstructions from growth increments too compressed to be otherwise accessible (e.g., Helser et al. 2018, Maggiano et al. 2019). Likewise, while the precise temperature significance of elemental concentrations is often unclear, intra-annual variation can be quickly and easily visualized (de Winter et al. 2017). Finally, while we focus on geochemical records here, recent work suggests that crystal orientations of modern bivalve nacre as revealed by a suite of new microscopy techniques correlate with the $\delta^{18}\text{O}$ values of shell determined using SIMS (Cartwright et al. 2020, Gilbert et al. 2017, Olson et al. 2012), offering the potential for a structural paleothermometer that can reveal seasonality without geochemical analysis.

PROCESSING SCLEROCRONOLOGIC ISOTOPE DATA

Data from accretionary organisms reveal oxygen isotope profiles that typically exhibit cyclic increases and decreases with distance along the sampled transect (**Figures 3 and 4**). To maximize the seasonal information gleaned from these profiles, the y axis must be converted from $\delta^{18}\text{O}$ to temperature and (ideally) the x axis from distance into time. Such transforms require knowledge of or assumptions about (a) the chemistry of the seawater at the time of growth and (b) the intra- and interannual growth patterns of the organism.

Translation to Paleotemperatures

Oxygen isotope values can be converted to temperature using a variety of transfer functions, the choice of which depends on the mineralogy and taxonomic affiliation of the sampled specimen. However, regardless of which equation is chosen (for a comprehensive review of temperature equations, see Grossman 2012), they all relate the same three variables: the isotopic composition of the carbonate ($\delta^{18}\text{O}_{\text{carb}}$), the isotopic composition of the seawater from which the carbonate precipitated ($\delta^{18}\text{O}_{\text{sw}}$), and temperature (T). This presents a conundrum whereby only one value is known ($\delta^{18}\text{O}_{\text{carb}}$) and two are unknown ($\delta^{18}\text{O}_{\text{sw}}$ and T). Paleotemperature estimates from $\delta^{18}\text{O}_{\text{carb}}$ therefore require either an assumption about or independent constraint on the $\delta^{18}\text{O}_{\text{sw}}$ value, which can be difficult in deep time.

Today, the global average $\delta^{18}\text{O}_{\text{sw}}$ value is 0‰, but this varies over geologic time as a function of ice volume. Pore fluid data from drill cores provide an anchor point of +1‰ during the Last Glacial Maximum (Schrag et al. 2002), and mass balance equations using the isotopic composition and volume of modern ice sheets suggest a value of -1‰ in an ice-free world (Shackleton & Kennett 1975). However, the $\delta^{18}\text{O}$ value of ocean surface water also varies spatially by as much as 5‰ today, a function of the balance between evaporation and precipitation, modified by local contributions from runoff (LeGrande & Schmidt 2006). While a broad latitudinal trend exists, there are notable deviations, particularly in coastal regions and semienclosed seas; this is particularly important, as these are the locations from which most paleoseasonal proxy data derive (**Figure 1a**). $\delta^{18}\text{O}_{\text{sw}}$ can be approximated in deep time by superimposing today's latitudinal trend on the estimated global average (Zachos et al. 1994) or using an independent proxy to constrain SST and then back calculate $\delta^{18}\text{O}_{\text{sw}}$ at key points in Earth history from the $\delta^{18}\text{O}_{\text{carb}}$ data (e.g., Bergmann et al. 2018, Bougeois et al. 2018, Hollis et al. 2012, Lear et al. 2000, Woelders et al. 2018). Still farther back in time, the pattern of decreasing $\delta^{18}\text{O}_{\text{carb}}$ values with increasing age (Veizer & Prokoph 2015, Veizer et al. 1986) introduces the potential for Phanerozoic-scale secular change in the $\delta^{18}\text{O}$ of the entire hydrosphere (Defliese 2021, Galili et al. 2019, Jaffrés et al. 2007, Vérard & Veizer 2019); if true, this implies that paleotemperatures calculated from $\delta^{18}\text{O}$ values will be progressively overestimated with increasing age unless independent estimates of $\delta^{18}\text{O}_{\text{sw}}$ can be obtained.

In addition to uncertainty in the mean annual $\delta^{18}\text{O}_{\text{sw}}$ value, paleoseasonal studies need also contend with the possibility of seasonally variable $\delta^{18}\text{O}_{\text{sw}}$ (e.g., Conroy et al. 2017, McConnell et al. 2009, Strauss et al. 2012). Unlike SST, where sinusoidal intra-annual oscillation is largely predicted by theory, subannual $\delta^{18}\text{O}_{\text{sw}}$ responds also to weather phenomena such as hurricanes, atmospheric rivers, and meltwater pulses, making it more difficult to predict. This is once again important to consider, as most seasonal proxy records come from nearshore environments that are influenced by such phenomena. Many ESMs now incorporate isotope systematics (e.g., Brady et al. 2019, Tindall et al. 2010, Zhou et al. 2008, Zhu et al. 2020), which can provide estimates of intra-annual and spatial variability in $\delta^{18}\text{O}_{\text{sw}}$ in deep time. ESMs or proxy data can also be used to constrain the seasonal precipitation cycle, which can then be used to gauge whether

large seasonal variations in $\delta^{18}\text{O}_{\text{sw}}$ are to be anticipated (e.g., Judd et al. 2019, Tierney et al. 2020a). Just as with mean annual $\delta^{18}\text{O}_{\text{sw}}$, independent temperature proxies can also help constrain the seasonal temperature cycle, or at least the seasonal extremes, permitting back calculation of subannual $\delta^{18}\text{O}_{\text{sw}}$. Keating-Bitonti et al. (2011), for example, used $\delta^{18}\text{O}$ profiles to a priori identify carbonate from seasonal extremes and then pooled sampled material from those intervals to circumvent the sample-size limitations of clumped isotopes analysis, leading to the recognition of seasonal $\delta^{18}\text{O}_{\text{sw}}$ variation. Methodological advances (Meckler et al. 2014) in combination with fast-growing shells make direct seasonal temperature and hence $\delta^{18}\text{O}_{\text{sw}}$ determinations possible using Δ_{47} (Caldarescu et al. 2021, de Winter et al. 2021). While the uncertainty on these measurements remains large, the approach can be used to establish a probabilistic distribution of summer and winter $\delta^{18}\text{O}_{\text{sw}}$ values from which the higher-precision $\delta^{18}\text{O}_{\text{carb}}$ temperature estimates can be derived.

Removing the Influence of Growth

Intra-annual variation in growth rate is propagated into the geochemical record such that with evenly spaced sampling, more isotope data come from the season of maximum accretion (**Figure 4b**). This has consequences for reconstruction of the seasonal cycle and MAT in deep time. This limitation can be partially circumvented by calculating climate statistics from individual seasonal extremes rather than using all data, but in order to reconstruct the full annual temperature cycle and compare it to, for example, seasonal outputs from ESMs, distance along the growth axis must be converted into time using computational routines.

Algebraic/statistical approaches. Typical variables of interest in paleoclimate studies include MAT, MART, and the temperature of seasonal extremes (summer and winter). Estimating these parameters does not necessarily require that data be transformed from distance into time—in fact, many paleoseasonality studies do not do this. However, there is no standardized method for calculating these values, and several important factors can bias them.

MART is most simply estimated by taking the difference between the warmest and coldest inferred temperatures from across the entire data set. However, given the interannual variability observed across most isotope profiles and the stochastic variability observed in most instrumental climate records, this is likely to overestimate the typical seasonal range (Wilkinson & Ivany 2002). Alternatively, MART can be calculated by taking the difference between the means of all local maxima and minima interpreted to be seasonal extremes, or by calculating the mean of the differences between adjacent or all pairs of inferred seasonal extremes. These approaches are advantageous as they allow for determination of statistical uncertainty around the estimates of seasonal extremes and overall MART, making the metrics more robust. However, as discussed above, intra-annual and ontogenetic changes in extension rate will lead to variable under- or overestimates of the temperature during the season of minimum growth and thus dampen the overall inferred seasonal range. Likewise, MAT can be calculated in a variety of ways, the most straightforward method being the average of all data points. However, concentration of data in one season over another biases the result toward the season of maximum growth. The mean of the midpoints between all pairs of adjacent seasonal extremes is an improvement, but it is still subject to bias associated with preferential growth in one season over another.

While these statistical approaches can provide insight into important paleoclimate metrics, they rely solely on data from the seasonal extremes, overlooking the added insight from the remainder of a high-resolution data set, and all are subject to seasonally biased growth. Further, without a time component, the metrics are difficult to contextualize with ESM outputs, which generally report seasonality as the difference between mean monthly values or multimonth

seasonal averages [e.g., June–July–August (JJA) and January–February–March (JFM)]. Regardless of the approach taken, authors should be clear about how they determine their reported climate metrics and any associated error terms.

Computational approaches. A variety of methods, written in different coding languages and with varying degrees of complexity, can be used to temporally align $\delta^{18}\text{O}$ profiles, ameliorating the impact of seasonally biased growth. The simplest approach is to linearly interpolate between anchor points with known temporal significance, such as those defined by seasonal extremes (de Brauwere et al. 2009, Müller et al. 2015). Although this can yield realistic results in taxa with low variability in intra-annual growth rates (e.g., Titschack et al. 2010), the approach is sensitive to the choice of anchor point (de Brauwere et al. 2009), and the assumption of constant growth between anchor points is biologically unrealistic.

Most of the more complex numerical approaches are predicated on the same governing principle that seasonal SSTs generally oscillate sinusoidally, and hence if growth rates were constant throughout the year (and $\delta^{18}\text{O}_{\text{sw}}$ largely constant or in phase with SSTs), then isotope profiles would also be sinusoidal. In reality though, isotope profiles are often cusped or skewed (e.g., **Figure 4**), and these deviations from the predicted sinusoidal shape reflect the influence of changing growth rates over the year. The assumption of sinusoidal temperature variability thus creates a target function (cf. de Brauwere et al. 2009) against which to transform the data. In their most basic form, data can be temporally aligned by iteratively fitting sine curves to successive moving windows of a seasonally resolved data set (Wilkinson & Ivany 2002). This approach, however, still assumes that growth rate is constant over the individual windows of data being fit, results are sensitive to the user-selected size of the window, and it either neglects the impact of changes in extension rate on the phase of the sinusoid (Wilkinson & Ivany 2002) or requires the presumption of a constant sinusoidal amplitude across the entire time series (De Ridder et al. 2007).

Borrowing a page from the sedimentary age modeling community (Martinson et al. 1982, Judd et al. 2018) bypass the assumption of constant growth by introducing a mapping function (cf. de Brauwere et al. 2009) that relates the isotope profiles to the sinusoidal target function. Here, growth rate is represented by a skewed sinusoidal mapping function, mirroring the commonly observed asymmetry of intra-annual growth (e.g., Hallmann et al. 2009). Negative growth values, based on the position and amplitude of the growth sinusoid, are fixed at zero, allowing the function to incorporate growth cessations. The user inputs (a) the isotope data or isotope-derived SSTs and associated distance values, (b) the positions of year markers as inferred from isotope minima or maxima or the positions of visible growth bands, and (c) the upper and lower bounds on permissible skewness of the growth sinusoid (values between 0 and 100, where 50 indicates no skew) and of the amplitude (i.e., MART) and position (i.e., MAT) of the temperature sinusoid (in per mil if using isotope data or degrees Celsius if data are already converted to temperatures). The period of both the temperature and growth functions is fixed at 365 days, and the phase of both functions evolves naturally. Predicted $\delta^{18}\text{O}_{\text{carb}}$ profiles from discrete years are iteratively calculated by generating temperature and growth rate functions with randomized parameters between the prescribed bounds using a shuffled complex evolution algorithm (Duan et al. 1992) that are then compared with the observed $\delta^{18}\text{O}_{\text{carb}}$ data. Best-fit solutions are those that minimize the root mean square error between the predicted and observed $\delta^{18}\text{O}_{\text{carb}}$ profiles. The GRATISS (Growth Rate and Temporal Alignment of Isotopic Serial Samples) model, originally written in MATLAB and freely available on GitHub (Judd et al. 2018), has been translated to R with added functionality that propagates error throughout the routine (N.J. de Winter, unpublished article).

The GRATISS model has several advantages even beyond accounting for variable and asymmetric intra-annual growth and growth hiatuses. First, each sampled year is evaluated

independently, meaning that climatological assumptions do not carry over from one year to the next, thus permitting time series analysis of natural interannual variability. Second, in addition to temporally aligning the data, the routine generates growth rate functions for each year, enabling the parallel interpretation of growth rate, either over the ontogeny of an individual or en toto by averaging the profiles to generate a mean growth rate profile for a specific taxon. Third, once temporally aligned, individual years of data can be stacked onto the same annual cycle and fit with a sinusoid and its associated uncertainty bounds; climate metrics (e.g., MAT, MART) can then be calculated and uncertainty constrained (see examples below). This approach therefore has a distinct advantage over the purely statistical approaches in that all data points contribute to the overall calculation, rather than just the seasonal extremes. Sampling at least 30 discrete years from a given time interval, ideally from two or more taxa with different seasons of minimum and maximum growth or at least multiple specimens of the same taxon, lends confidence that the resulting curve represents a true climatology.

Advantages notwithstanding, GRATISS or its R equivalent only works in environments where temperature can be assumed to vary sinusoidally (an assumption required for all approaches using a sinusoid as their target function). The validity of this presumption has been demonstrated using instrumental data in a variety of settings (e.g., Judd et al. 2018, Wilkinson & Ivany 2002). The R^2 (coefficient of determination) value of climatological mean monthly SSTs (Hirahara et al. 2014) for all ocean grid cells fit with a sinusoid further endorses the fidelity of this assumption (**Figure 2c**), but highlights that deviations do occur in the modern high latitudes and in the tropics. Additionally, restricted basins with seasonal thermoclines can exhibit skewed seasonal curves, especially at depth (e.g., Schöne et al. 2005b), so it is important to consider the paleoenvironment from which the data come and whether the assumption might be violated. Additionally, the approach is sensitive to input bounds on the amplitude and position of the temperature function. If the bounds are too relaxed, the model can cluster the data during a single seasonal extreme rather than distribute them throughout the year, overestimating the amplitude of seasonality and spuriously imposing protracted growth cessations. Alternatively, if the bounds are too restrictive, the model cannot incorporate growth hiatuses, leading to an underestimate of MART. Generally, best results are achieved by setting the lower and upper bounds to 10% less and more, respectively, than the observed amplitude and position of the data for a given year, although some trial and error may be required. Ultimately, however, if data from multiple years are pooled onto a single annual cycle, a single anomalous year will become evident and be less likely to impart a large influence on the overall climate metrics.

INTERPRETATION (AND MISINTERPRETATION) OF SEASONALLY RESOLVED DATA

Acknowledging uncertainties related to water composition or growth rate, the consistent cyclic nature of oxygen isotope profiles from accretionary carbonates clearly reflects environmental temperature variation. For paleoclimate work, the challenge is determining how best to interpret the seasonal data. Several cautions apply.

One Shell Is Rarely Enough

Because of the time- (and money-) intensive nature of microsampling work, many publications report seasonally resolved data from only one or a few individuals. Single-shell records can be useful in certain circumstances, such as testing for a seasonal growth bias or establishing the annual nature of growth banding to inform future sampling. In some cases, single records can point to a need for specific interpretations of data with respect to, for example, freshwater influx.

But their real impact is in the context of paleoecology and evolution, where just one specimen can be enough to resolve long-standing debates or highlight unexpected phenomena (e.g., Buick & Ivany 2004, Jones & Gould 1999, Moss et al. 2021). Given the spatial and temporal variability that characterizes the climate system and the uncertainties associated with proxy data, a single seasonal record is insufficient to characterize mean conditions represented by a stratigraphic horizon. Modern climatologies are generally 30-year averages, and a single MAT estimate from, for example, IODP cores often represents an average over thousands of years. Seasonally resolved isotope records even from long-lived taxa rarely exceed a decade (but for a spectacular exception in shallow time, see Schöne et al. 2005a). Therefore, to compare paleoseasonal metrics with these types of MAT estimates, the seasonal data set should consider the timescales of variation inherent to each. A number of shorter records from different individuals within the target stratigraphic interval are more useful than a single long record (Carré et al. 2012), as this approach better captures interannual variation over longer timescales. In the absence of specific hypothesis-testing scenarios, we encourage the community to strive for these larger and strategically designed data sets.

Most Data Do Not Come from the Open Ocean

Nearly all seasonal $\delta^{18}\text{O}$ data come from macrofossils collected in outcrop, and hence reflect coastal or epeiric settings (**Figure 1a**). Judd et al. (2020) demonstrate that modern SSTs in nearshore environments exhibit large deviations from the zonal mean due to meridional advection from gyre circulation, and epeiric sea settings today are statistically warmer and more seasonal than open-ocean settings at comparable latitudes as a result of the lower heat capacity of continents and shallower depths of mixing in the water column. Therefore, even when isotope-derived temperatures clearly reflect SSTs, those values are unlikely to be representative of zonal mean values. In data-poor time intervals, latitudinal gradients are often calculated without accounting for these biases, and MAT and MART values from similar paleolatitudes but disparate paleoceanographic regimes are sometimes compared, leading to spurious interpretations. With the volume and geographic coverage of proxy data now available, particularly in the Cenozoic, anomalous regions are now more frequently recognized and zonal heterogeneity considered. For example, Eocene SST data from the Pacific (Hollis et al. 2012) and Atlantic (Douglas et al. 2014) sectors of the Southern Ocean are significantly offset from one another, with the latter yielding paleotemperatures far cooler than the former. However, ESMs suggest that such heterogeneity can be achieved due to the influences of a warm proto-East Australian Current and a change to the location of deep-water formation in the Ross Sea (Douglas et al. 2014, Hollis et al. 2012), and analysis of modern SSTs suggests that such heterogeneity is to be expected in subdivided high-latitude ocean basins, analogous to the modern boreal high latitudes (Judd et al. 2019). The resulting strong zonal heterogeneity in the Southern Ocean prior to establishment of the Antarctic Circumpolar Current therefore illustrates the difficulty of generalizing latitudinal gradients from one location alone and the danger in assuming proxy values from the same latitude must always agree with one another. Data assimilation, a statistical technique that integrates proxy observations, both annually and seasonally, with ESMs offers a promising new method for reconciling proxy-proxy and proxy-model disagreements (Hughes & Ammann 2009, Tierney et al. 2020b).

Most Accretionary Marine Macrofauna Are Benthic

As water depth increases, the amplitude of seasonal temperature variation decreases (Prandle & Lane 1995). This poses a challenge, as paleodepth is only qualitatively and indirectly constrained in the sedimentary record (Peters & Loss 2012). In shallow, well-mixed settings where conditions

at the bottom closely mirror those at the surface (Austin et al. 2006), depth is generally not a concern, but in deeper or stratified water columns, the range of bottom water temperature variation can be substantially less than that at the surface. Mollusks living below a seasonal thermocline, for example, will not capture the full seasonal range of SSTs even if growth is continuous throughout the year (Austin et al. 2006). As well, attenuation of seasonal range has, itself, a seasonal bias—winter temperatures generally remain consistent while summer temperatures cool with increasing depth, progressively lowering both MAT and MART (Austin et al. 2006, Prandle & Lane 1995, Wilkinson & Ivany 2002). Uncertainty related to paleodepth is not limited to accretionary organisms; many planktonic foraminifera live well below the surface and some move vertically through ontogeny (Pearson 2012), and debate remains over whether some TEX₈₆ data reflect subsurface conditions (Inglis & Tierney 2020). The nearshore nature of most paleoseasonal records lends confidence that they reflect SSTs, but the influence of paleodepth on isotope-derived seasonality should be considered (e.g., via sedimentary structures or faunal assemblages) and data sets compared to others from similar facies to establish robust spatiotemporal patterns. Where possible, concomitant analyses of co-occurring mixed-layer planktonic foraminifera might help determine whether the benthic record is likely to be biased and by how much. Because winter temperatures are less impacted by water depth, comparison of winter extremes alone in settings with questionable paleodepths can still provide insight on SSTs across geography or through time.

THE PROMISE OF PALEOSEASONALITY

Seasonally resolved stable isotope profiles from recent and fossil materials have appeared with increasing frequency in the published literature over the past several decades (**Figure 1b**). Despite their growing prevalence, the novelty of sclerochronologic data and the challenges that accompany them mean that these records are often interpreted in isolation and largely overlooked in proxy-model comparison projects or broad paleoceanographic and paleoclimatological syntheses. These are missed opportunities. Again, the seasonal cycle is how biology—including people—experiences climate, so these records from the past are integral to making climate change relevant to the public and for helping people understand projected future conditions. Below, we reanalyze three published data sets from the Eocene using updated statistical and computational approaches to highlight the fidelity of paleoseasonal data and illustrate the opportunities they offer for a deeper understanding of past climates.

Seasonality in Space and Time

Perhaps the most compelling of questions that can be asked with paleoseasonality data is how the seasonal cycle has varied across space and through time, when surface conditions and continental configurations were unlike those today. Theoretically, with adequate coverage and internally consistent taxon selection and sampling methodology, seasonal climate metrics can be evaluated within a temporal or geographic framework to reconstruct trends or patterns that can reveal, for example, large-scale ocean circulation patterns or the seasonal underpinnings that drive changes in MAT. Despite this potential, concerns that localized phenomena (e.g., variable salinity) dominate the signal have caused many to shy away from interpreting their data in a larger context. Sessa et al. (2012) explore the consistency and replicability of proxy-based seasonal metrics by generating seasonal data from shells of the same taxon of fossil bivalve collected from multiple localities in a single time plane and facies exposed along hundreds of kilometers of paleocoastline in the Eocene of the US Gulf Coastal Plain (**Figure 5**). We revisit their data using statistical approaches (as described above in the section titled Algebraic/Statistical Approaches) to test whether

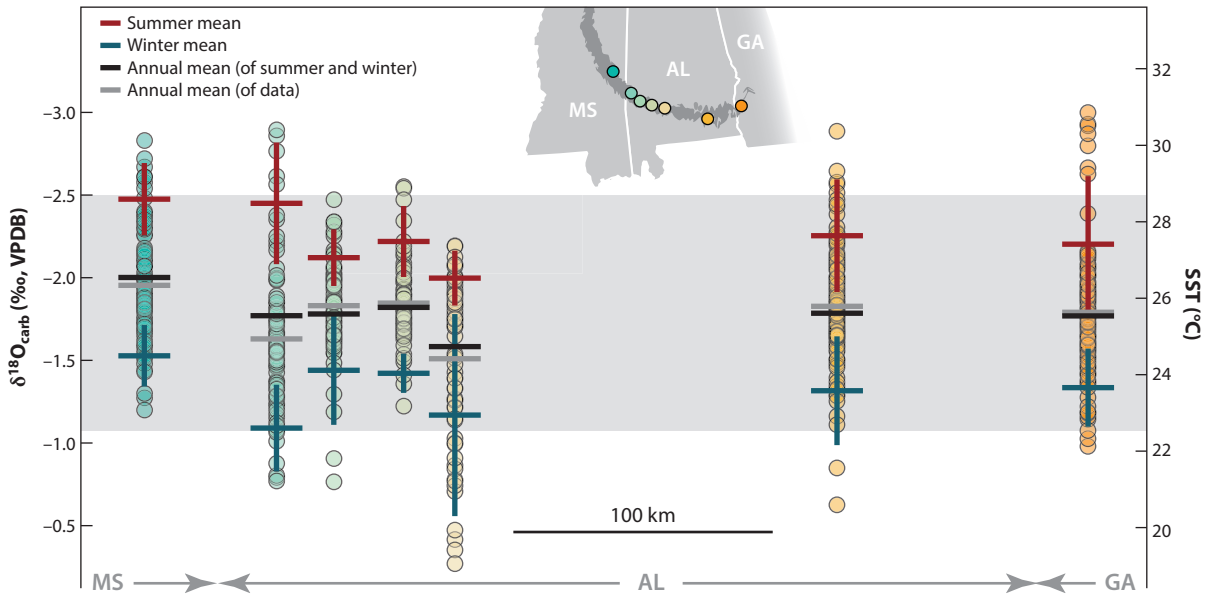


Figure 5

Oxygen isotope data from serially sampled venericardiine bivalves collected along an east-to-west trajectory in the early Eocene Bashi Marl on the US Gulf Coast. Data points reflect all individual bivalve measurements pooled from multiple specimens and/or over multiple years from each of the seven sampling localities, with colors corresponding to the locations shown on the inset map; two closely spaced sites in Mississippi are pooled into one. Seasonal extremes in the original profiles were identified based on sequential peaks and troughs in the $\delta^{18}\text{O}$ data and averaged across shells to yield summer (red) and winter (blue) means from each location. Annual averages (black) represent the arithmetic mean of all data points. SST (right axis) was calculated using the aragonite equation of Grossman & Ku (1986) assuming a $\delta^{18}\text{O}_{\text{sw}}$ value of -0.36 (Sessa et al. 2012). The gray band shows the full range of temperatures encompassed by all the summer and winter mean values. Abbreviations: $\delta^{18}\text{O}_{\text{carb}}$, $\delta^{18}\text{O}$ of carbonate; $\delta^{18}\text{O}_{\text{sw}}$, $\delta^{18}\text{O}$ of the seawater; SST, sea surface temperature; VPDB, Vienna Pee Dee Belemnite. Data from Sessa et al. (2012) and one shell originally published by Kobashi et al. (2004); figure adapted from Ivany (2012).

local variability overwhelms regional signal. Seasonal extremes were identified from 639 isotope measurements derived from 18 shells across seven different sampling locations, and summer and winter means and standard deviations were calculated for each site. Annual averages were calculated from both the arithmetic means of all samples at a location and the means of the summer and winter values at each location (Figure 5). Despite the expected intershell variability, population averages are impressively consistent, in terms of both MAT and MART, from place to place along the coast (Figure 5). One-way analysis of variance (ANOVA) testing of summer and winter values by specimen suggests that the seasonal extremes of individual shells are statistically distinct from one another (p -values $\ll 0.0001$); however, mean summer values and mean winter values by site are statistically indistinguishable (p -values > 0.05). Importantly, data sets such as these demonstrate that (a) while single years or specimens may exhibit anomalous values, with sufficient samples and specimens the population averages converge on similar values; and (b) microsampled records from shelf macrofossils can indeed preserve a regional seasonal climate signal and therefore contribute meaningfully to assessments of climate through time.

With the knowledge that seasonal data from large data sets are statistically consistent across broad regions, these kinds of data can and should be integrated with MAT proxy data and used to investigate spatial and temporal trends in MAT and MART that inform about process. For example, there are now a good number of seasonally resolved records spanning the Atlantic Ocean

during the early and middle Eocene. These records could be compiled into a coherent framework to elucidate the causal processes that give rise to observed patterns. In the modern ocean, for example, coastal SSTs are controlled by gyre circulation, allowing different dynamical regimes to be fingerprinted by characteristic MAT and MART combinations (Judd et al. 2020); regions of upwelling tend to be both colder and less seasonal, while confluence regions where two currents meet are colder but more seasonal. When viewed in this light, compilations of spatially distributed seasonal data offer a means of reconstructing paleoceanographic dynamics that might not be possible otherwise given the resolution and requisite boundary conditions of ESMs (e.g., fixed position of the zero-stress wind curl, which largely controls the latitudinal extent of gyres). Likewise, seasonal data from a single geographic region over an interval of large-scale global change will demonstrate how, or if, seasonal range changes with changing MAT, providing insight into the mechanisms responsible.

Validating Earth System Models

Seasonal data can also play a key role in assessing the fidelity of climate models. While most preindustrial ESM simulations now converge on similar MAT solutions, models diverge in their reconstruction of seasonal cycles over both land (Gasson et al. 2014) and sea (Judd et al. 2020). These discrepancies are amplified in deep time, as uncertainties in boundary conditions grow and differences in model physics are made more apparent (Gasson et al. 2014). To explore the extent to which ESMs can capture the annual cycle of both SSTs and $\delta^{18}\text{O}_{\text{sw}}$, we compare seasonal ESM outputs from an early Eocene isotope-enabled Community Earth System Model (iCESM) simulation (Zhu et al. 2019) with serially sampled bivalve data of the same age from the Hatchetigbee Formation of the US Gulf Coastal Plain [31.66°N, 88.09°W (Ivany et al. 2004b, Keating-Bitonti et al. 2011)] (**Figure 6**). Following the approach of Tierney et al. (2020a), where the comparison was first drawn, we forward model mean monthly $\delta^{18}\text{O}_{\text{carb}}$ values by extracting SST and $\delta^{18}\text{O}_{\text{sw}}$ from the eight closest grid cells to the paleolocation of the sampling site and rearranging the aragonite temperature equation to solve for $\delta^{18}\text{O}_{\text{carb}}$, propagating the variance observed between the grid cells. We then quantify the proxy-derived annual SST cycle using a statistically rigorous Monte Carlo resampling approach we first introduce here, which accounts for uncertainty in both the x and y direction and propagates error throughout to yield the single best-fit solution to all data with an associated envelope of uncertainty.

Shell $\delta^{18}\text{O}$ profiles for each defined year are first transformed from the distance domain into time using the GRATAISS model (Judd et al. 2018). Although the model does not quantify uncertainty in the date assignments of each data point, analysis of modern data with known growth and temperature indicates that on average, date assignments have a 1σ error of about 1 week. For each of the 344 data points spanning 31 years of growth, we generate an ensemble of possible date values, drawing from a normal distribution with a mean value of the initial date assignment from the GRATAISS model and a standard deviation of 7 days. Similarly, we then create a $\delta^{18}\text{O}_{\text{carb}}$ ensemble that accounts for analytical uncertainty around the initial value ($1\sigma = 0.05\%$). We then pool all data into the same 1-year reference frame using Julian day assignments and reconstruct the climatological seasonal cycle 25,000 times. At each iteration, we randomly select 75% of the data and, for each of those points, draw paired x values from the date ensemble and y values from the $\delta^{18}\text{O}_{\text{carb}}$ ensemble. The resulting values are then fit with a sinusoid with a fixed period of 365 days, and the R^2 value of the fit is recorded. We eliminate all fits except for those with R^2 values at or above the ninety-fifth percentile, presuming that those are the solutions with the most realistic age and $\delta^{18}\text{O}_{\text{carb}}$ values. The full range of those remaining 1,250 fits defines the uncertainty envelope, and their mean value defines the ultimate climatological solution for the annual cycle.

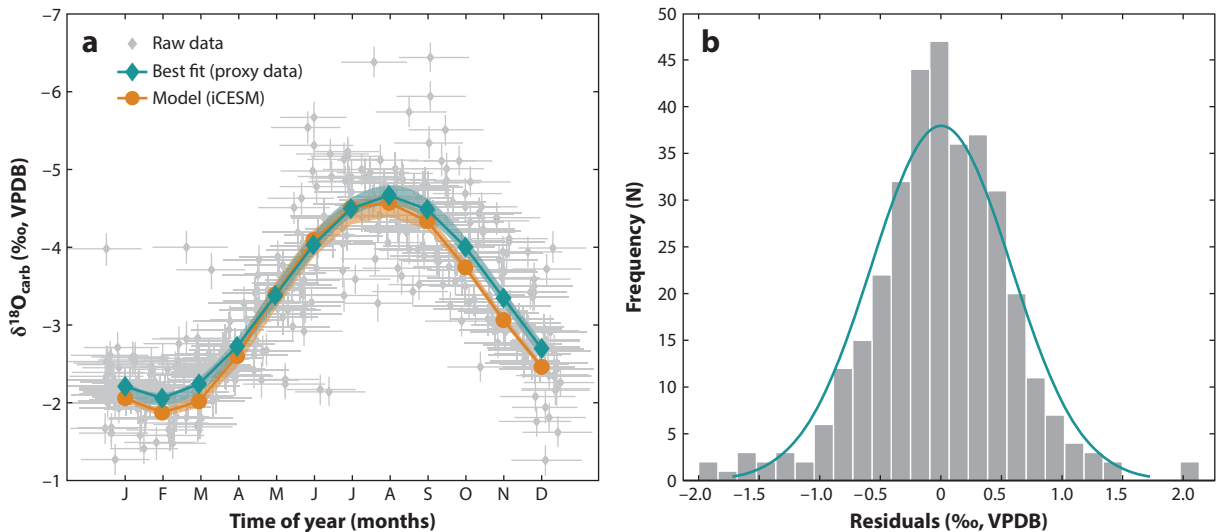


Figure 6

(a) Comparison of sine-fit seasonally resolved $\delta^{18}\text{O}_{\text{carb}}$ data from early Eocene venericardiine bivalves from the Hatchetigbee Formation of the US Gulf Coastal Plain (Ivany et al. 2004b, Keating-Bitonti et al. 2011) and forward modeled $\delta^{18}\text{O}_{\text{carb}}$ using the isotope-enabled iCESM climate model (Zhu et al. 2020), modified after Tierney et al. (2020a). Gray diamonds show the raw isotope data, which were temporally aligned using the GRATISS model (Judd et al. 2018). Data were fit with a sinusoid with a fixed period of 365 days via a Monte Carlo resampling approach ($N = 25,000$; see text); horizontal and vertical lines show the full range of date and analytical uncertainty considered, respectively. (b) Residuals from the best-fit sinusoid of panel a. Abbreviations: $\delta^{18}\text{O}_{\text{carb}}$, $\delta^{18}\text{O}$ of carbonate; GRATISS, Growth Rate and Temporal Alignment of Isotopic Serial Samples; iCESM, isotope-enabled Community Earth System Model; VPDB, Vienna Pee Dee Belemnite.

The agreement between the forward modeled mean monthly $\delta^{18}\text{O}_{\text{carb}}$ values (derived only from iCESM) and the independent processed proxy data is impressive (**Figure 6a**), lending confidence to both the model fidelity and the regional applicability of seasonally resolved isotope data. The climatological proxy signal is better constrained by pooling multiple years and specimens and accounting for uncertainty through the application of robust statistical and computational methods; as with modern instrumental data (e.g., Judd et al. 2018), residuals from the fit are normally distributed (**Figure 6b**). Likewise, comparing mean monthly iCESM outputs, rather than annual averages, with the proxy data adds more data points and dimensions with which to interrogate the efficacy of the SST and isotope physics governing the ESM. Note that in this case, the best solution is one in which both temperature and $\delta^{18}\text{O}_{\text{SW}}$ vary seasonally, similar to that inferred from a multiproxy comparison (Keating-Bitonti et al. 2011). Agreement of proxy and model in this situation, which is somewhat less than straightforward, lends strong support to the value of seasonally resolved data and the power of an integrated approach. In this example, the proxy and model values agree well with one another, but this will not always be the case with different ESMs and sampling locations. Such comparisons, particularly using spatial compilations of seasonal data, may therefore help elucidate proxy-model mismatches and identify models that more accurately capture the seasonal cycle as well as MAT.

Identifying Biased Mean Annual Temperature

An important additional context in which seasonally resolved data can contribute to deep-time climate studies is by contextualizing the bulk data that comprise the majority of large-scale or

long-term studies. While it is not practical to obtain seasonally resolved data for hundreds of individuals across a time transect, high-resolution sampling from targeted intervals can give insights into the climatological significance of existing MAT time series or identify seasonal biases in other proxy data. For example, whole-shell data from two genera of bivalves in the Eocene section of Antarctica yield different isotope values despite consistently occurring in the same samples (Ivany et al. 2008). However, microsampling of only 4 specimens (out of 187 shells sampled for MAT) revealed that one genus grew preferentially during the winter, explaining its more positive $\delta^{18}\text{O}$ values. This too demonstrates the potential for conflation of temporal climate signals—real temperature change can be masked by a taxon tracking its preferred habitat or by disproportionate changes in MAT and MART through time. The absence of change in mean proxy composition over time or in space could mean that temperature is constant, or it could instead reflect a change in the season of growth or depth habitat of the organism to accommodate changing conditions (Jonkers & Kučera 2017); conversely, large changes in bulk values over time could be inflated if changes in, for example, summer temperatures, are larger than the concomitant change in MAT (as is observed in many modern environments). Without seasonally resolved data, constancy in average proxy composition can therefore be easily erroneously interpreted.

We explore this further by comparing serially sampled bivalve data from the middle Eocene of Seymour Island, Antarctica (Judd et al. 2019), with TEX_{86} data from the same section (Douglas et al. 2014) and the iCESM simulation used above (Zhu et al. 2019) to demonstrate that seasonal biases in high-latitude MAT data are not limited to accretionary organisms (**Figure 7**). In this example, the analyses were carried out in temperature space; mean monthly SSTs were extracted from the nine grid cells defining the northeastern coastline of the Antarctic Peninsula, and TEX_{86} -derived SSTs were estimated using the BAYSPAR (BAYesian SPATIally-varying Regression) calibration (Tierney & Tingley 2014). Following the approach above, we temporally aligned $\delta^{18}\text{O}$ values from seven shells representing two genera of bivalve and 32 years of growth and quantified the climatological seasonal cycle using a similar Monte Carlo resampling approach to account for uncertainties. A date ensemble for each of the 302 data points was calculated as above, and an SST ensemble was generated by accounting for uncertainty in $\delta^{18}\text{O}_{\text{sw}}$, informed by the iCESM values. Consistent with proxy- and model-derived evidence for a more or less equable precipitation regime, seasonal differences in the iCESM $\delta^{18}\text{O}_{\text{sw}}$ from the same grid cells used to extract SST were smaller than cell-to-cell differences in the mean annual value (0.16‰ and 0.38‰, respectively), suggesting that interannual differences are less significant than the uncertainty in the annual value. The SST ensemble therefore assumes a constant $\delta^{18}\text{O}_{\text{sw}}$ value for each shell but is drawn from a broad distribution of possible annual values. As above, random subsets of 75% of the data were iteratively fit 25,000 times, with paired values pulled from the age and SST ensembles, and the solution and uncertainty envelope defined by fits with R^2 values at or above the ninety-fifth percentile (**Figure 7a**).

We observe excellent agreement between $\delta^{18}\text{O}_{\text{carb}}$ - and model-derived summer SSTs, although winter SSTs are nearly 3°C colder in the ESM, yielding a larger MART and colder MAT than indicated by the proxy data. Interestingly, the seasonal range in the iCESM decreases quickly in a northward trend along the Peninsula (**Figure 7c**), indicating that perhaps the model is missing—or misplacing—certain aspects of circulation in the region. What is even more striking, however, is the agreement between mean austral summer (JFM) SSTs from the $\delta^{18}\text{O}$ - and model-derived curves with the TEX_{86} -derived values (**Figure 7b**). The TEX_{86} proxy is calibrated to core tops (Tierney & Tingley 2014), where modern high-latitude SST seasonality is low, so it is perhaps unsurprising that a seasonal bias has not been detected; however, it is theoretically reasonable to assume that given the highly seasonal nature of productivity in these environments, a seasonal bias might propagate onto the production of the biomarker. Although a high-latitude summertime bias

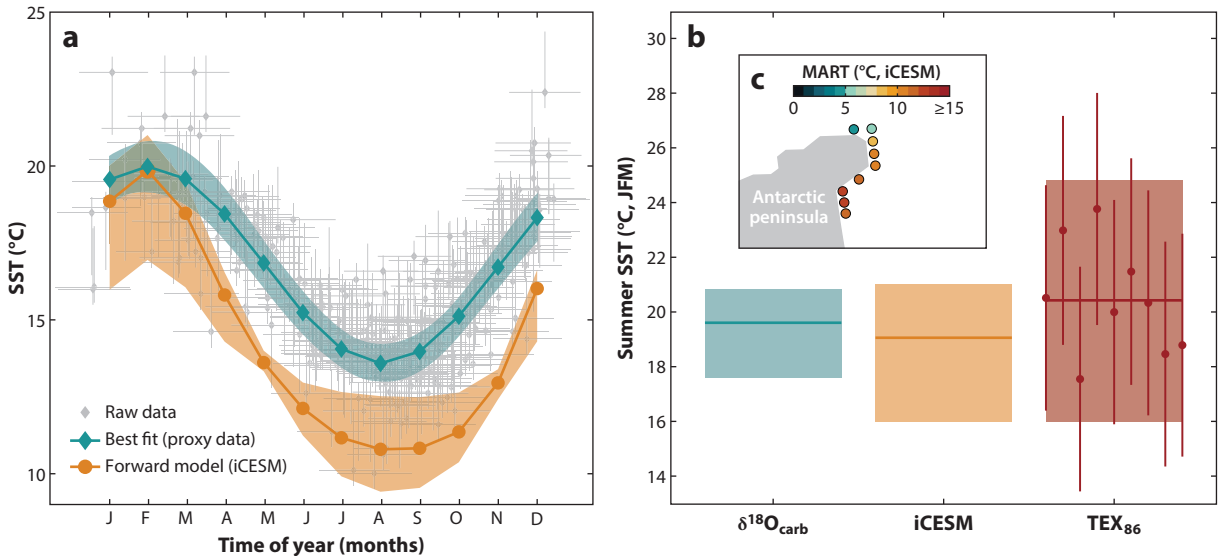


Figure 7

(a) Comparison of sine-fit seasonally resolved $\delta^{18}\text{O}$ - and iCESM- derived SSTs from the middle Eocene of Seymour Island, Antarctica (Judd et al. 2019, Zhu et al. 2020). Gray diamonds show discrete estimates of SST from serially sampled bivalves, which were temporally aligned using the GRATAISS model (Judd et al. 2018). Data were fit with a sinusoid with a fixed period of 365 days via a Monte Carlo resampling approach ($N = 25,000$); horizontal and vertical lines show the full range of date and SST uncertainties considered, respectively. (b) Comparison of austral summer (JFM) SSTs from the best-fit sine and modeled values in panel a and the TEX_{86} -derived SSTs also from Seymour Island (Douglas et al. 2014), calculated using BAYSPAR (Tierney & Tingley 2014). (c) Map showing the paleolocations of the nine grid cells used from iCESM to estimate SST and create $\delta^{18}\text{O}_{\text{sw}}$ distributions, colored by MART. Abbreviations: $\delta^{18}\text{O}_{\text{carb}}$, $\delta^{18}\text{O}$ of carbonate; BAYSPAR, BAYesian SPAtially-varying Regression; GRATAISS, Growth Rate and Temporal Alignment of Isotopic Serial Samples; iCESM, isotope-enabled Community Earth System Model; JFM, January-February-March; MART, mean annual range of temperature; SST, sea surface temperature.

in TEX_{86} has been proposed (e.g., Davies et al. 2019, Hollis et al. 2012), this example represents the first time that such a bias has been quantified, made possible only through the use of seasonally resolved data. Such seasonal biases are not limited to TEX_{86} and are likely location and time dependent; seasonally resolved proxy records therefore hold the key to elucidating proxy-proxy and proxy-model mismatches over a wide range of timescales.

A Proposal for Community-Driven Research?

The promise and potential of paleoseasonal data as described above call for a systematic survey to evaluate the fidelity of these kinds of data in capturing broad spatiotemporal patterns in SSTs in the modern ocean. Small-scale, internally consistent studies in the rock record such as those described above offer confidence that meaningful seasonal data can be recovered, interface with ESMs, and contribute to a better understanding of regional MAT. However, it is as yet unclear whether broadly distributed data from different taxa generated by different researchers in different ways can be integrated to yield a framework within which to study seasonal temperatures across ocean basins, environments, or latitudes. Existing seasonal records are few but not altogether rare in the Modern. Such data could be compiled to investigate the degree to which they, in aggregate, reflect the instrumental record of SSTs as seen in, for example, **Figure 2** and the paired MAT and MART patterns revealed by Judd et al. (2020). Key regions could be targeted for data collection and monitoring so as to fill gaps and test predicted gradients. Do the expected broad patterns

emerge from the data, or are they hopelessly complicated by diverse methodologies, depth-related bias, and local environmental heterogeneity? How many records, over how many years, and of what resolution, are needed to confidently establish a pattern in different types of settings? A compilation of this scope represents a significant investment of time and is best accomplished through a coordinated effort across the research community. We enthusiastically endorse such an effort moving forward. Given a sufficient quantity and quality of data, the signal is bound to emerge from the noise.

CONCLUSIONS

Accretionary skeletal records are the only climate archive able to consistently offer quantitative records of the seasonal temperature cycle and how it changes with MAT in deep time. Like all proxies, extracting and interpreting the paleoclimatic significance of chemical variations in these structures comes with challenges, but the technical and computational tools are now available with which to generate and analyze large, internally consistent, and broadly deployed data sets that can reveal robust spatiotemporal climate patterns in deep Earth history. These data can interface with ESMs to evaluate which models more accurately reproduce seasonal patterns in the past and therefore hopefully in the future, and with MAT data to bring greater clarity to proxy bias, address proxy-model mismatch and aid in holistic interpretations of ancient climates and dynamical regimes. The paleoclimate community is well positioned to take advantage of seasonally resolved data—we encourage researchers to span the disciplinary gaps too often present between the paleoceanographic, climate modeling, and sclerochronologic communities in order to reap the benefits afforded by these records.

DISCLOSURE STATEMENT

The authors are not aware of any affiliations, memberships, funding, or financial holdings that might be perceived as affecting the objectivity of this review.

ACKNOWLEDGMENTS

We thank Bruce Wilkinson, James Muirhead, Jess Tierney, Tripti Bhattacharya, Kau Thirumalai, Kacey Lohmann, and Meps for inspiration, feedback, and assistance with aspects of this review. The manuscript is stronger thanks to the thoughtful and thorough feedback provided by an anonymous reviewer. Published data reanalyzed here were originally generated during research supported by PLR-1543031 and EAR-0719645 from the National Science Foundation and 40418-G2 from the American Chemical Society, each to Ivany. Judd is supported by the PhanTASTIC Postdoctoral Fellowship, funded by Roland and Debra Sauermann.

LITERATURE CITED

- Addino MS, Alvarez MF, Brey T, Iribarne O, Lomovasky BJ. 2019. Growth changes of the stout razor clam *Tagelus plebeius* (Lightfoot, 1786) under different salinities in SW Atlantic estuaries. *J. Sea Res.* 146:14–23
- Affek H. 2012. Clumped isotope paleothermometry: principles, applications, and challenges. See Ivany & Huber 2012, pp. 101–14
- Arthur MA, Williams DF, Jones DS. 1983. Seasonal temperature-salinity changes and thermocline development in the mid-Atlantic Bight as recorded by the isotopic composition of bivalves. *Geology* 11:655–59
- Austin WEN, Cage AG, Scourse JD. 2006. Mid-latitude shelf seas: a NW European perspective on the seasonal dynamics of temperature, salinity and oxygen isotopes. *Holocene* 16:937–47

- Baldini JUL, Lechleitner FA, Breitenbach SFM, van Hunen J, Baldini LM, et al. 2021. Detecting and quantifying palaeoseasonality in stalagmites using geochemical and modelling approaches. *Quat. Sci. Rev.* 254:106784
- Beard JA, Ivany LC, Runnegar B. 2015. Gradients in seasonality and seawater oxygen isotopic composition along the early Permian Gondwanan coast, SE Australia. *Earth Planet. Sci. Lett.* 425:219–31
- Beelaerts V, De Ridder F, Schmitz N, Bauwens M, Pintelon R. 2010. Time-series reconstruction from natural archive data with the averaging effect taken into account. *Math. Geosci.* 42:705–22
- Bergmann KD, Finnegan S, Creel R, Eiler JM, Hughes NC, et al. 2018. A paired apatite and calcite clumped isotope thermometry approach to estimating Cambro-Ordovician seawater temperatures and isotopic composition. *Geochim. Cosmochim. Acta* 224:18–41
- Berry WB, Barker RM. 1968. Fossil bivalve shells indicate longer month and year in Cretaceous than present. *Nature* 217:938–39
- Botsyun S, Ehlers TA. 2021. How can climate models be used in paleoelevation reconstructions? *Front. Earth Sci.* 9:28
- Bougeois L, Dupont-Nivet G, de Rafélis M, Tindall JC, Proust J-N, et al. 2018. Asian monsoons and aridification response to Paleogene sea retreat and Neogene westerly shielding indicated by seasonality in Paratethys oysters. *Earth Planet. Sci. Lett.* 485:99–110
- Brady E, Stevenson S, Bailey D, Liu Z, Noone D, et al. 2019. The connected isotopic water cycle in the Community Earth System Model version 1. *J. Adv. Model. Earth Syst.* 11:2547–66
- Brand U. 2004. Carbon, oxygen and strontium isotopes in Paleozoic carbonate components: an evaluation of original seawater-chemistry proxies. *Chem. Geol.* 204:23–44
- Brand U, Azmy K, Bitner M, Logan A, Zuschin M, et al. 2013. Oxygen isotopes and MgCO₃ in brachiopod calcite and a new paleotemperature equation. *Chem. Geol.* 359:23–31
- Brassell SC, Eglinton G, Marlowe IT, Pflaumann U, Sarnthein M. 1986. Molecular stratigraphy: a new tool for climatic assessment. *Nature* 320:129–33
- Buick DP, Ivany LC. 2004. 100 years in the dark: extreme longevity of Eocene bivalves from Antarctica. *Geology* 32:921–24
- Burke K, Williams J, Chandler M, Haywood A, Lunt D, Otto-Bliesner B. 2018. Pliocene and Eocene provide best analogs for near-future climates. *PNAS* 115:13288–93
- Caldarescu DE, Sadatzki H, Andersson C, Schäfer P, Fortunato H, Meckler AN. 2021. Clumped isotope thermometry in bivalve shells: a tool for reconstructing seasonal upwelling. *Geochim. Cosmochim. Acta* 294:174–91
- Campana SE. 1999. Chemistry and composition of fish otoliths: pathways, mechanisms and applications. *Mar. Ecol. Prog. Ser.* 188:263–97
- Carré M, Cheddadi R. 2017. Seasonality in long-term climate change. *Quaternaire* 28:173–77
- Carré M, Sachs J, Wallace J, Favier C. 2012. Exploring errors in paleoclimate proxy reconstructions using Monte Carlo simulations: paleotemperature from mollusk and coral geochemistry. *Clim. Past* 8:433–50
- Cartwright JH, Checa AG, Sainz-Díaz CI. 2020. Nacre is a liquid-crystal thermometer of the oceans. *ACS Nano* 14:9277–81
- Chen S, Gagnon AC, Adkins JF. 2018. Carbonic anhydrase, coral calcification and a new model of stable isotope vital effects. *Geochim. Cosmochim. Acta* 236:179–97
- CLIMAP. 1981. *Seasonal reconstructions of the Earth's surface at the last glacial maximum*. Tech. Rep. MC-36, Geol. Soc. Am., Boulder, CO
- Conroy JL, Thompson DM, Cobb KM, Noone D, Rea S, Legrande AN. 2017. Spatiotemporal variability in the δ¹⁸O-salinity relationship of seawater across the tropical Pacific Ocean. *Paleoceanography* 32:484–97
- Crowley TJ, Short DA, Mengel JG, North GR. 1986. Role of seasonality in the evolution of climate during the last 100 million years. *Science* 231:579–84
- Darnaude AM, Sturrock A, Trueman CN, Mouillot D, Campana SE, Hunter E. 2014. Listening in on the past: What can otolith δ¹⁸O values really tell us about the environmental history of fishes? *PLOS ONE* 9:e108539
- Davies A, Hunter SJ, Gréselle B, Haywood AM, Robson C. 2019. Evidence for seasonality in early Eocene high latitude sea-surface temperatures. *Earth Planet. Sci. Lett.* 519:274–83

- de Brauwere A, De Ridder F, Pintelon R, Schoukens J, Dehairs F. 2009. A comparative study of methods to reconstruct a periodic time series from an environmental proxy record. *Earth-Sci. Rev.* 95:97–118
- De Ridder F, de Brauwere A, Pintelon R, Schoukens J, Dehairs F, et al. 2007. Comment on: Paleoclimatic inference from stable isotope profiles of accretionary biogenic hardparts—a quantitative approach to the evaluation of incomplete data, by BH Wilkinson, LC Ivany. 2002. *Palaeogeogr. Palaeoclimatol. Palaeoecol.* 185, 95–114. *Palaeogeogr. Palaeoclimatol. Palaeoecol.* 248:473–76
- de Winter NJ, Müller IA, Kocken IJ, Thibault N, Ullmann CV, et al. 2021. Absolute seasonal temperature estimates from clumped isotopes in bivalve shells suggest warm and variable greenhouse climate. *Commun. Earth Environ.* 2:121
- de Winter NJ, Sinnesael M, Makarona C, Vansteenberge S, Claeys P. 2017. Trace element analyses of carbonates using portable and micro-X-ray fluorescence: performance and optimization of measurement parameters and strategies. *J. Anal. At. Spectrom.* 32:1211–23
- Defliese WF. 2021. The impact of Snowball Earth glaciation on ocean water $\delta^{18}\text{O}$ values. *Earth Planet. Sci. Lett.* 554:116661
- DeLong KL, Quinn TM, Taylor FW, Shen C-C, Lin K. 2013. Improving coral-base paleoclimate reconstructions by replicating 350 years of coral Sr/Ca variations. *Palaeogeogr. Palaeoclimatol. Palaeoecol.* 373:6–24
- Disspain MC, Ulm S, Gillanders BM. 2016. Otoliths in archaeology: methods, applications and future prospects. *J. Archaeol. Sci. Rep.* 6:623–32
- Dolman AM, Kunz T, Groeneveld J, Laepple T. 2021. Estimating the timescale-dependent uncertainty of paleoclimate records—a spectral approach. Part II: application and interpretation. *Clim. Past* 17:825–41
- Douglas PMJ, Affek HP, Ivany LC, Houben AJP, Sijp WP, et al. 2014. Pronounced zonal heterogeneity in Eocene southern high-latitude sea surface temperatures. *PNAS* 111:6582–87
- Duan Q, Sorooshian S, Gupta V. 1992. Effective and efficient global optimization for conceptual rainfall-runoff models. *Water Resour. Res.* 28:1015–31
- Edwards CT, Jones CM, Quinton PC, Fike DA. 2022. Oxygen isotope ($\delta^{18}\text{O}$) trends measured from Ordovician conodont apatite using secondary ion mass spectrometry (SIMS): implications for paleothermometry studies. *GSA Bull.* 134:261–74
- Eiler JM. 2011. Paleoclimate reconstruction using carbonate clumped isotope thermometry. *Quat. Sci. Rev.* 30:3575–88
- Evans D, Müller W, Oron S, Renema W. 2013. Eocene seasonality and seawater alkaline earth reconstruction using shallow-dwelling large benthic foraminifera. *Earth Planet. Sci. Lett.* 381:104–15
- Frailé I, Mulitza S, Schulz M. 2009. Modeling planktonic foraminiferal seasonality: implications for sea-surface temperature reconstructions. *Mar. Micropaleontol.* 72:1–9
- Galili N, Shemesh A, Yam R, Brailovsky I, Sela-Adler M, et al. 2019. The geologic history of seawater oxygen isotopes from marine iron oxides. *Science* 365:469–73
- Gasson E, Lunt DJ, DeConto R, Goldner A, Heinemann M, et al. 2014. Uncertainties in the modelled CO_2 threshold for Antarctic glaciation. *Clim. Past* 10:451–66
- Gilbert PU, Bergmann KD, Myers CE, Marcus MA, DeVol RT, et al. 2017. Nacre tablet thickness records formation temperature in modern and fossil shells. *Earth Planet. Sci. Lett.* 460:281–92
- Gillikin DP, Lorrain A, Navez J, Taylor JW, Andre L, et al. 2005. Strong biological controls on Sr/Ca ratios in aragonitic marine bivalve shells. *Geochem. Geophys. Geosyst.* 6:Q05009
- Goodwin DH, Schone BR, Dettman DL. 2003. Resolution and fidelity of oxygen isotopes as paleotemperature proxies in bivalve mollusk shells: models and observations. *Palaïos* 18:110–25
- Groeneveld J, Ho SL, Mackensen A, Mohtadi M, Laepple T. 2019. Deciphering the variability in Mg/Ca and stable oxygen isotopes of individual foraminifera. *Paleoceanogr. Palaeoclimatol.* 34:755–73
- Grossman EL. 2012. Applying oxygen isotope paleothermometry in deep time. See Ivany & Huber 2012, pp. 39–67
- Grossman EL, Ku T-L. 1986. Oxygen and carbon isotope fractionation in biogenic aragonite: temperature effects. *Chem. Geol.* 59:59–74
- Hallmann N, Burchell M, Schöne BR, Irvine GV, Maxwell D. 2009. High-resolution sclerochronological analysis of the bivalve mollusk *Saxidomus gigantea* from Alaska and British Columbia: techniques for revealing environmental archives and archaeological seasonality. *J. Archaeol. Sci.* 36:2353–64

- Helser TE, Kastelle CR, McKay JL, Orland IJ, Kozdon R, Valley JW. 2018. Evaluation of micromilling/conventional isotope ratio mass spectrometry and secondary ion mass spectrometry of $\delta^{18}\text{O}$ values in fish otoliths for sclerochronology. *Rapid Commun. Mass Spectrom.* 32:1781–90
- Hemingway J, Henkes G. 2021. A distributed activation energy model for clumped isotope bond reordering in carbonates. *Earth Space Sci. Open Arch.* 41. <https://www.essoar.org/doi/10.1002/essoar.10504096.2>
- Henkes GA, Passey BH, Grossman EL, Shenton BJ, Yancey TE, Pérez-Huerta A. 2018. Temperature evolution and the oxygen isotope composition of Phanerozoic oceans from carbonate clumped isotope thermometry. *Earth Planet. Sci. Lett.* 490:40–50
- Herbert TD. 2014. Alkenone paleotemperature determinations. In *Treatise on Geochemistry*, ed. HD Holland, KK Turekian, pp. 399–433. Oxford, UK: Elsevier. 2nd ed.
- Hirahara S, Ishii M, Fukuda Y. 2014. Centennial-scale sea surface temperature analysis and its uncertainty. *J. Clim.* 27:57–75
- Hollis CJ, Taylor KWR, Handley L, Pancost RD, Huber M, et al. 2012. Early Paleogene temperature history of the Southwest Pacific Ocean: reconciling proxies and models. *Earth Planet. Sci. Lett.* 349–350:53–66
- Hughes M, Ammann C. 2009. The future of the past—an earth system framework for high resolution paleoclimatology: editorial essay. *Clim. Change* 94:247–59
- Immenhauser A, Schoene BR, Hoffmann R, Niedermayr A. 2016. Mollusc and brachiopod skeletal hard parts: intricate archives of their marine environment. *Sedimentology* 63:1–59
- Inglis GN, Tierney JE. 2020. *The TEX86 Paleotemperature Proxy*. Cambridge, UK: Cambridge Univ. Press
- Ingram BL, Conrad ME, Ingle JC. 1996. Stable isotope and salinity systematics in estuarine waters and carbonates: San Francisco Bay. *Geochim. Cosmochim. Acta* 60:455–67
- Ivany LC. 2012. Reconstructing paleoseasonality from accretionary skeletal carbonates: challenges and opportunities. See Ivany & Huber 2012, pp. 133–65
- Ivany LC, Huber BT, eds. 2012. *Reconstructing Earth's Deep-Time Climate: The State of the Art in 2012*, Vol. 18. Boulder, CO: Paleontol. Soc.
- Ivany LC, Lohmann KC, Blake DB, Hasiuk F, Aronson RB, et al. 2008. Eocene climate record of a high southern latitude continental shelf: Seymour Island, Antarctica. *Geol. Soc. Am. Bull.* 120:659–78
- Ivany LC, Patterson WP, Lohmann KC. 2000. Cooler winters as a possible cause of mass extinctions at the Eocene/Oligocene boundary. *Nature* 407:887–90
- Ivany LC, Peters SE, Wilkinson BH, Lohmann KC, Reimer BA. 2004a. Composition of the early Oligocene ocean from coral stable isotope and elemental chemistry. *Geobiology* 2:97–106
- Ivany LC, Wilkinson BH, Lohmann KC, Johnson ER, McElroy BJ, Cohen GJ. 2004b. Intra-annual isotopic variation in *Venericardia* bivalves: implications for early Eocene temperature, seasonality, and salinity on the US Gulf Coast. *J. Sediment. Res.* 74:7–19
- Jaffrés JBD, Shields GA, Wallmann K. 2007. The oxygen isotope evolution of seawater: a critical review of a long-standing controversy and an improved geological water cycle model for the past 3.4 billion years. *Earth-Sci. Rev.* 83:83–122
- Jain S, Lall U, Mann ME. 1999. Seasonality and interannual variations of Northern Hemisphere temperature: equator-to-pole gradient and ocean–land contrast. *J. Clim.* 12:1086–100
- Jones DS. 1983. Sclerochronology: reading the record of the molluscan shell. *Am. Sci.* 71:384–91
- Jones DS, Gould SJ. 1999. Direct measurement of age in fossil *Gryphaea*: the solution to a classic problem in heterochrony. *Paleobiology* 25:158–87
- Jones DS, Quitmyer IR. 1996. Marking time with bivalve shells: oxygen isotopes and season of annual increment formation. *Palaios* 11:340–46
- Jones PD, New M, Parker DE, Martin S, Rigor IG. 1999. Surface air temperature and its changes over the past 150 years. *Rev. Geophys.* 37:173–99
- Jonkers L, Kučera M. 2017. Quantifying the effect of seasonal and vertical habitat tracking on planktonic foraminifera proxies. *Clim. Past* 13:573–86
- Judd EJ, Bhattacharya T, Ivany LC. 2020. A dynamical framework for interpreting ancient sea surface temperatures. *Geophys. Res. Lett.* 47:e2020GL089044
- Judd EJ, Ivany LC, DeConto RM, Halberstadt ARW, Miklus NM, et al. 2019. Seasonally resolved proxy data from the Antarctic Peninsula support a heterogeneous middle Eocene Southern Ocean. *Paleoceanogr. Paleoclimatol.* 34:787–99

- Judd EJ, Wilkinson BH, Ivany LC. 2018. The life and time of clams: derivation of intra-annual growth rates from high-resolution oxygen isotope profiles. *Palaeogeogr. Palaeoclimatol. Palaeoecol.* 490:70–83
- Keating-Bitonti CR, Ivany LC, Affek HP, Douglas P, Samson SD. 2011. Warm, not super-hot, temperatures in the early Eocene subtropics. *Geology* 39:771–74
- Kelson JR, Huntington KW, Breecker DO, Burgener LK, Gallagher TM, et al. 2020. A proxy for all seasons? A synthesis of clumped isotope data from Holocene soil carbonates. *Quat. Sci. Rev.* 234:106259
- Kennish MJ. 1980. Shell microgrowth analysis: *Mercenaria mercenaria* as a type example for research in population dynamics. See Rhoads & Lutz 1980, pp. 255–94
- Killam DE, Clapham ME. 2018. Identifying the ticks of bivalve shell clocks: seasonal growth in relation to temperature and food supply. *Palaios* 33:228–36
- Kobashi T, Grossman EL, Dockery DT, Ivany LC. 2004. Water mass stability reconstructions from greenhouse (Eocene) to icehouse (Oligocene) for the northern Gulf Coast continental shelf (USA). *Paleoceanography* 19:PA1022
- Kung EC, Bryson RA, Lenschow DH. 1964. Study of a continental surface albedo on the basis of flight measurements and structure of the earth's surface cover over North America. *Mon. Weather Rev.* 92:543–64
- Lea DW. 2014. 8.14 Elemental and isotopic proxies of past ocean temperatures. In *Treatise on Geochemistry*, ed. HD Holland, KK Turekian, pp. 373–97. Oxford, UK: Elsevier. 2nd ed.
- Lea DW, Mashiotto TA, Spero HJ. 1999. Controls on magnesium and strontium uptake in planktonic foraminifera determined by live culturing. *Geochim. Cosmochim. Acta* 63:2369–79
- Lear CH, Elderfield H, Wilson PA. 2000. Cenozoic deep-sea temperatures and global ice volumes from Mg/Ca in benthic foraminiferal calcite. *Science* 287:269–72
- LeGrande AN, Schmidt GA. 2006. Global gridded data set of the oxygen isotopic composition in seawater. *Geophys. Res. Lett.* 33:L12604
- Linzmeier BJ. 2019. Refining the interpretation of oxygen isotope variability in free-swimming organisms. *Swiss J. Palaeontol.* 138:109–21
- Ljungström G, Langbehn TJ, Jørgensen C. 2021. Light and energetics at seasonal extremes limit poleward range shifts. *Nat. Clim. Change* 11:530–36
- Lowenstein TK, Hönisch B. 2012. The use of Mg/Ca as a seawater temperature proxy. See Ivany & Huber 2012, pp. 85–100
- Lutz RA, Rhoads DC. 1980. Growth patterns within the molluscan shell. See Rhoads & Lutz 1980, pp. 203–54
- Maggiano CM, White CD, Stern RA, Peralta JS, Longstaffe FJ. 2019. Focus: oxygen isotope microanalysis across incremental layers of human bone: exploring archaeological reconstruction of short term mobility and seasonal climate change. *J. Archaeolog. Sci.* 111:105028
- Markwick PJ. 1998. Fossil crocodylians as indicators of Late Cretaceous and Cenozoic climates; implications for using palaeontological data in reconstructing palaeoclimate. *Palaeogeogr. Palaeoclimatol. Palaeoecol.* 137:205–71
- Marshall JF, McCulloch MT. 2002. An assessment of the Sr/Ca ratio in shallow water hermatypic corals as a proxy for sea surface temperature. *Geochim. Cosmochim. Acta* 66:3263–80
- Martinson DG, Menke W, Stoffa P. 1982. An inverse approach to signal correlation. *J. Geophys. Res.* 87(B6):4807–18
- Matsuoka J, Kano A, Oba T, Watanabe T, Sakai S, Seto K. 2001. Seasonal variation of stable isotopic compositions recorded in a laminated tufa, SW Japan. *Earth Planet. Sci. Lett.* 192:31–44
- Matthews T, Mullan D, Wilby RL, Broderick C, Murphy C. 2016. Past and future climate change in the context of memorable seasonal extremes. *Clim. Risk Manag.* 11:37–52
- McConnaughey T. 1989. ¹³C and ¹⁸O isotopic disequilibrium in biological carbonates II. *In vitro* simulation of kinetic isotope effects. *Geochim. Cosmochim. Acta* 53:163–71
- McConnell MC, Thunell RC, Lorenzoni L, Astor Y, Wright JD, Fairbanks R. 2009. Seasonal variability in the salinity and oxygen isotopic composition of seawater from the Cariaco Basin, Venezuela: implications for paleosalinity reconstructions. *Geochim. Geophys. Geosyst.* 10:Q06019
- Meckler AN, Ziegler M, Millán MI, Breitenbach SF, Bernasconi SM. 2014. Long-term performance of the Kiel carbonate device with a new correction scheme for clumped isotope measurements. *Rapid Commun. Mass Spectrom.* 28:1705–15

- Meehl GA, Richter JH, Teng H, Capotondi A, Cobb K, et al. 2021. Initialized Earth System prediction from subseasonal to decadal timescales. *Nat. Rev. Earth Environ.* 2:340–57
- Metcalf B, Feldmeijer W, Ganssen GM. 2019. Oxygen isotope variability of planktonic foraminifera provide clues to past upper ocean seasonal variability. *Paleoceanogr. Paleoclimatol.* 34:374–93
- Miyaji T, Tanabe K, Matsushima Y, Sato Si, Yokoyama Y, Matsuzaki H. 2010. Response of daily and annual shell growth patterns of the intertidal bivalve *Phacosoma japonicum* to Holocene coastal climate change in Japan. *Palaeogeogr. Palaeoclimatol. Palaeoecol.* 286:107–20
- Moon LR, Judd EJ, Thomas J, Ivany LC. 2021. Out of the oven and into the fire: unexpected preservation of the seasonal $\delta^{18}\text{O}$ cycle following heating experiments on shell carbonate. *Palaeogeogr. Palaeoclimatol. Palaeoecol.* 562:110115
- Moss DK, Ivany LC, Jones DS. 2021. Fossil bivalves and the sclerochronological reawakening. *Paleobiology* 2021:1–23
- Müller P, Taylor MH, Klicpera A, Wu HC, Michel J, Westphal H. 2015. Food for thought: mathematical approaches for the conversion of high-resolution sclerochronological oxygen isotope records into sub-annually resolved time series. *Palaeogeogr. Palaeoclimatol. Palaeoecol.* 440:763–76
- Olson IC, Kozdon R, Valley JW, Gilbert PU. 2012. Mollusk shell nacre ultrastructure correlates with environmental temperature and pressure. *J. Am. Chem. Soc.* 134:7351–58
- Pannella G, MacClintock C. 1968. Biological and environmental rhythms reflected in molluscan shell growth. In *Paleobiological Aspects of Growth and Development*, ed. DB Macurda Jr., pp. 64–81. Menasha, WI: Banta
- Passey BH, Henkes GA. 2012. Carbonate clumped isotope bond reordering and geospeedometry. *Earth Planet. Sci. Lett.* 351–352:223–36
- Pearson PN. 2012. Oxygen isotopes in foraminifera: overview and historical review. See Ivany & Huber 2012, pp. 1–38
- Pérez-Huerta A, Cusack M, Jeffries TE, Williams CT. 2008. High resolution distribution of magnesium and strontium and the evaluation of Mg/Ca thermometry in Recent brachiopod shells. *Chem. Geol.* 247:229–41
- Peters SE, Loss DP. 2012. Storm and fair-weather wave base: a relevant distinction? *Geology* 40:511–14
- Pisias NG, Roelofs A, Weber M. 1997. Radiolarian-based transfer functions for estimating mean surface ocean temperatures and seasonal range. *Paleoceanography* 12:365–79
- Poulain C, Gillikin DP, Thébault J, Munaron JM, Bohn M, et al. 2015. An evaluation of Mg/Ca, Sr/Ca, and Ba/Ca ratios as environmental proxies in aragonite bivalve shells. *Chem. Geol.* 396:42–50
- Prandle D, Lane A. 1995. The annual temperature cycle in shelf seas. *Cont. Shelf Res.* 15:681–704
- Purton LMA, Brasier MD. 1999. Giant protist *Nummulites* and its Eocene environment: life span and habitat insights from $\delta^{18}\text{O}$ and $\delta^{13}\text{C}$ data from *Nummulites* and *Venericardia*, Hampshire basin, UK. *Geology* 27:711–14
- Radtke R, Showers W, Moksness E, Lenz P. 1996. Environmental information stored in otoliths: insights from stable isotopes. *Mar. Biol.* 127:161–70
- Rayner NA. 2003. Global analyses of sea surface temperature, sea ice, and night marine air temperature since the late nineteenth century. *J. Geophys. Res.* 108(D14):4407
- Rhoads DC, Lutz RA, eds. 1980. *Skeletal Growth of Aquatic Organisms*. New York: Plenum
- Roy T, He X, Lin P, Beck HE, Castro C, Wood EF. 2020. Global evaluation of seasonal precipitation and temperature forecasts from NMME. *J. Hydrometeorol.* 21:2473–86
- Rye DM, Sommer MAI. 1980. Reconstructing paleotemperature and paleosalinity regimes with oxygen isotopes. See Rhoads & Lutz 1980, pp. 169–202
- Sato S. 1995. Spawning periodicity and shell microgrowth patterns of the venerid bivalve *Phacosoma japonicum* (Reeve, 1850). *Véliger* 38:61–72
- Schöne BR, Fiebig J, Pfeiffer M, Gleß R, Hickson J, et al. 2005a. Climate records from a bivalved Methuselah (*Arctica islandica*, Mollusca; Iceland). *Palaeogeogr. Palaeoclimatol. Palaeoecol.* 228:130–48
- Schöne BR, Lega J, Flessa KW, Goodwin DH, Dettman DL. 2002. Reconstructing daily temperatures from growth rates of the intertidal bivalve mollusk *Chione cortezi* (northern Gulf of California, Mexico). *Palaeogeogr. Palaeoclimatol. Palaeoecol.* 184:131–46

- Schöne BR, Pfeiffer M, Pohlmann T, Siegismund F. 2005b. A seasonally resolved bottom-water temperature record for the period AD 1866–2002 based on shells of *Arctica islandica* (Mollusca, North Sea). *Int. J. Climatol.* 25:947–62
- Schöne BR, Surge D. 2012. Part N, Revised, Volume 1, Chapter 14: Bivalve sclerochronology and geochemistry. *Treatise Online* 46:1–24
- Schöne BR, Zhang Z, Radermacher P, Thébault J, Jacob DE, et al. 2011. Sr/Ca and Mg/Ca ratios of ontogenetically old, long-lived bivalve shells (*Arctica islandica*) and their function as paleotemperature proxies. *Palaeogeogr. Palaeoclimatol. Palaeoecol.* 302:52–64
- Schouten S, Hopmans EC, Schefuß E, Sinninghe Damste JS. 2002. Distributional variations in marine crenarchaeotal membrane lipids: a new tool for reconstructing ancient sea water temperatures? *Earth Planet. Sci. Lett.* 204:265–74
- Schrag DP, Adkins JF, McIntyre K, Alexander JL, Hodell DA, et al. 2002. The oxygen isotopic composition of seawater during the Last Glacial Maximum. *Quat. Sci. Rev.* 21:331–42
- Seager R, Murtugudde R, Naik N, Clement A, Gordon N, Miller J. 2003. Air–sea interaction and the seasonal cycle of the subtropical anticyclones. *J. Clim.* 16:1948–66
- Sessa JA, Ivany LC, Schlossnagle T, Samson SD, Schellenberg SA. 2012. The fidelity of oxygen and strontium isotope values from shallow shelf settings: implications for temperature and age reconstructions. *Palaeogeogr. Palaeoclimatol. Palaeoecol.* 342–343:27–39
- Shackleton NJ, Kennett JP. 1975. Paleotemperature history of the Cenozoic and the initiation of Antarctic glaciation: oxygen and carbon isotope analyses in DSDP Sites 277, 279, and 281. *Initial Rep. Deep Sea Drill. Proj.* 74:743–55
- Strauss J, Grossman EL, DiMarco SF. 2012. Stable isotope characterization of hypoxia-susceptible waters on the Louisiana shelf: tracing freshwater discharge and benthic respiration. *Cont. Shelf Res.* 47:7–15
- Sunday JM, Bates AE, Dulvy NK. 2012. Thermal tolerance and the global redistribution of animals. *Nat. Clim. Change* 2:686–90
- Swart PK. 1983. Carbon and oxygen isotope fractionation in scleractinian corals: a review. *Earth-Sci. Rev.* 19:51–80
- Thirumalai K, Partin JW, Jackson CS, Quinn TM. 2013. Statistical constraints on El Niño Southern Oscillation reconstructions using individual foraminifera: a sensitivity analysis. *Paleoceanography* 28:401–12
- Tierney JE, Poulsen CJ, Montañez IP, Bhattacharya T, Feng R, et al. 2020a. Past climates inform our future. *Science* 370:eaay3701
- Tierney JE, Tingley MP. 2014. A Bayesian, spatially-varying calibration model for the TEX₈₆ proxy. *Geochim. Cosmochim. Acta* 127:83–106
- Tierney JE, Zhu J, King J, Malevich SB, Hakim GJ, Poulsen CJ. 2020b. Glacial cooling and climate sensitivity revisited. *Nature* 584:569–73
- Tindall J, Flecker R, Valdes P, Schmidt DN, Markwick P, Harris J. 2010. Modelling the oxygen isotope distribution of ancient seawater using a coupled ocean–atmosphere GCM: implications for reconstructing early Eocene climate. *Earth Planet. Sci. Lett.* 292:265–73
- Titschack J, Zuschin M, Spötl C, Baal C. 2010. The giant oyster *Hyotissa hyotis* from the northern Red Sea as a decadal-scale archive for seasonal environmental fluctuations in coral reef habitats. *Coral Reefs* 29:1061–75
- Urey HC. 1948. Oxygen isotopes in nature and in the laboratory. *Science* 108:489–96
- Urey HC, Lowenstam HA, Epstein S, McKinney CR. 1951. Measurement of paleotemperatures and temperatures of the Upper Cretaceous of England, Denmark, and the southeastern United States. *Geol. Soc. Am. Bull.* 62:399–416
- Valentine JW. 1983. Seasonality: effects in marine benthic communities. In *Biotic Interactions in Recent and Fossil Communities*, ed. MJS Tevesz, PL McCall, pp. 121–56. New York: Plenum
- Veizer J, Fritz P, Jones BG. 1986. Geochemistry of brachiopods: oxygen and carbon isotopic records of Phanerozoic oceans. *Geochim. Cosmochim. Acta* 50:1679–96
- Veizer J, Prokoph A. 2015. Temperatures and oxygen isotopic composition of Phanerozoic oceans. *Earth-Sci. Rev.* 146:92–104
- Vérard C, Veizer J. 2019. On plate tectonics and ocean temperatures. *Geology* 47:881–85

- Wefer G, Berger WH. 1980. Stable isotopes in benthic foraminifera: seasonal variation in large tropical species. *Science* 209:803–5
- Wefer G, Berger WH. 1991. Isotope paleontology: growth and composition of extant calcareous species. *Mar. Geol.* 100:207–48
- Wells JW. 1963. Coral growth and geochronometry. *Nature* 197:948–50
- Westerhold T, Marwan N, Drury AJ, Liebrand D, Agnini C, et al. 2020. An astronomically dated record of Earth's climate and its predictability over the last 66 million years. *Science* 369:1383–87
- Wilkinson BH, Ivany LC. 2002. Paleoclimatic inference from stable isotopic compositions of accretionary biogenic hardparts—a quantitative approach to the evaluation of incomplete data. *Palaeogeogr. Palaeoclimatol. Palaeoecol.* 185:95–114
- Williams DF, Arthur MA, Jones DS, Healy-Williams N. 1982. Seasonality and mean annual sea surface temperatures from isotopic and sclerochronological records. *Nature* 296:432–34
- Wit JC, Reichert G-J, Jung SJA, Kroon D. 2010. Approaches to unravel seasonality in sea surface temperatures using paired single-specimen foraminiferal $\delta^{18}\text{O}$ and Mg/Ca analyses. *Paleoceanography* 25:PA4220
- Witbaard R, Duineveld GC, Bergman M. 2001. The effect of tidal resuspension on benthic food quality in the southern North Sea. *Senckenberg. Marit.* 31:225–34
- Woelders L, Vellekoop J, Weltje GJ, de Nooijer L, Reichert G-J, et al. 2018. Robust multi-proxy data integration, using late Cretaceous paleotemperature records as a case study. *Earth Planet. Sci. Lett.* 500:215–24
- Wycech JB, Kelly DC, Kozdon R, Orland IJ, Spero HJ, Valley JW. 2018. Comparison of $\delta^{18}\text{O}$ analyses on individual planktic foraminifer (*Orbulina universa*) shells by SIMS and gas-source mass spectrometry. *Chem. Geol.* 483:119–30
- Zachos JC, Stott LD, Lohmann KC. 1994. Evolution of early Cenozoic marine temperatures. *Paleoceanography* 9:353–87
- Zander PD, Żarczyński M, Tylmann W, Rainford S-k, Grosjean M. 2021. Seasonal climate signals preserved in biochemical varves: insights from novel high-resolution sediment scanning techniques. *Clim. Past* 17:2055–71
- Zhou J, Poulsen C, Pollard D, White T. 2008. Simulation of modern and middle Cretaceous marine $\delta^{18}\text{O}$ with an ocean-atmosphere general circulation model. *Paleoceanography* 23:PA3223
- Zhu J, Poulsen CJ, Otto-Bliesner BL, Liu Z, Brady EC, Noone DC. 2020. Simulation of early Eocene water isotopes using an Earth system model and its implication for past climate reconstruction. *Earth Planet. Sci. Lett.* 537:116164
- Zhu J, Poulsen CJ, Tierney JE. 2019. Simulation of Eocene extreme warmth and high climate sensitivity through cloud feedbacks. *Sci. Adv.* 5:eaax1874